

---

Masters Theses

Student Theses and Dissertations

---

Spring 2015

## Neutronic analysis of light water Small Modular Reactor with flexible fuel configurations

Brendan Dsouza

Follow this and additional works at: [https://scholarsmine.mst.edu/masters\\_theses](https://scholarsmine.mst.edu/masters_theses)

 Part of the [Nuclear Engineering Commons](#)

Department:

---

### Recommended Citation

Dsouza, Brendan, "Neutronic analysis of light water Small Modular Reactor with flexible fuel configurations" (2015). *Masters Theses*. 7393.  
[https://scholarsmine.mst.edu/masters\\_theses/7393](https://scholarsmine.mst.edu/masters_theses/7393)

This thesis is brought to you by Scholars' Mine, a service of the Curtis Laws Wilson Library at Missouri University of Science and Technology. This work is protected by U. S. Copyright Law. Unauthorized use including reproduction for redistribution requires the permission of the copyright holder. For more information, please contact [scholarsmine@mst.edu](mailto:scholarsmine@mst.edu).

NEUTRONIC ANALYSIS OF LIGHT WATER SMALL MODULAR REACTOR  
WITH FLEXIBLE FUEL CONFIGURATIONS

By

BRENDAN DSOUZA

A THESIS

Presented to the Faculty of the Graduate School of the  
MISSOURI UNIVERSITY OF SCIENCE AND TECHNOLOGY

In Partial Fulfillment of the Requirements for the Degree

MASTER OF SCIENCE IN NUCLEAR ENGINEERING

2015

Approved by:

Ayodeji B. Alajo, Advisor  
Shoaib Usman  
Xin Liu



## ABSTRACT

The study was focused on the analysis of light water Small Modular Reactor (SMR) with flexible fuel configurations. The core design, based on the Westinghouse UO<sub>2</sub> SMR with less than 5% enrichment was developed using the Monte Carlo N-Particle (MCNP) code. Neutronics analyses of a reference core with UO<sub>2</sub> fuel was performed to characterize parameters such as the radial neutron flux profile, the maximum to average flux ratio, the reactivity coefficient and critical boron concentration at beginning of life; which confirmed good performance in comparison to a standard UO<sub>2</sub> based pressurized water reactor.

Using this uranium oxide (UOX) core as a reference, the SMR was then investigated with mixed oxide (MOX) and transuranic (TRU) fuels. The TRU fuel used was an inert matrix fuel with 8% UO<sub>2</sub> spent fuel as the fissile material and 92% Yttrium Stabilized Zirconia (YSZ) as the fertile inert matrix. The use of inert matrix enhanced the ability of the fuel to achieve better depletion. The results obtained for MOX and TRU fuels were also found to be within the requirements.

The burnup analysis for the actinides and the fission products for each of the oxide fueled cores was also determined which is necessary for the reactor criticality-safety design studies. The depletion analysis for MOX and TRU fuels indicated a higher fuel burn-up with an overall Pu<sup>239</sup> consumption of 54% for reactor grade MOX core, 74% for weapon grade MOX core and 94% for TRU core respectively. In conclusion, the results indicated a satisfactory behavior of SMR core with UOX, MOX and TRU fuels. To confirm the viability of this flexible fuel option, it is necessary to further validate this results and also analyze the core for its thermal-hydraulics behavior.

## ACKNOWLEDGEMENT

I would like to express my sincere gratitude to my advisor Dr. Ayodeji Alajo for his support and encouragement throughout this project. Thank you for your time and patience, in teaching me the MCNP code and also addressing the numerous doubts I had pertaining to the software which was crucial to my research work. It was with your immense knowledge, valuable insight and constant motivation that I was able to complete my thesis. I would also like to extend my gratitude to my committee members Dr. Shoaib Usman and Dr. Xin Liu, for their patience and valuable suggestions.

I would like to acknowledge all my friends and the MST Nuclear engineering faculty for all the help extended towards me during my master's program. A special thanks to Kirby Compton, Shaikat Galib, Manish Sharma and Raul Florez for helping me learn the MATLAB software which was a useful tool for my research work.

Finally, I would like to thank my family and my dearest sister Blanche Dsouza. It is because of their financial support, motivation and prayers that I was able to complete my graduate school.

## TABLE OF CONTENTS

	Page
ABSTRACT.....	iii
ACKNOWLEDGEMENT .....	iv
LIST OF FIGURES .....	vii
LIST OF TABLES.....	ix
NOMENCLATURE .....	x
 SECTION	
1. INTRODUCTION .....	1
1.1. SMALL NUCLEAR REACTORS .....	2
1.2. CURRENT STATUS OF SMR IN USA .....	3
1.3. RESEARCH OBJECTIVES .....	6
2. CORE MODEL AND METHODOLOGY .....	7
2.1. CORE GEOMETRY.....	7
2.2. FUEL ASSEMBLY CONFIGURATIONS .....	8
2.2.1. Uranium-oxide Fuel Assembly .....	9
2.2.2. Mixed-oxide Fuel Assembly.....	13
2.2.3. Transuranic Fuel Assembly .....	18
2.3. NEUTRON TRANSPORT CALCULATIONS .....	21
2.4. NEUTRONIC METHODOLOGY .....	22
2.4.1. Radial Neutron Flux Profile .....	22
2.4.2. Delayed Neutron Fraction.....	23

2.4.3. Control Rod.....	25
2.4.4. Temperature Reactivity Co-efficient .....	25
2.4.5. Critical Boron Concentration .....	27
2.4.6. Burn-up Calculations .....	27
2.4.6.1. Refueling strategy.....	29
2.4.6.2. Equilibrium cycle and nuclear spent fuel .....	29
3. RESULTS AND DISCUSSION .....	30
3.1. URANIUM-OXIDE FUEL.....	30
3.2. MIXED-OXIDE FUEL.....	39
3.3. TRANSURANIC FUEL .....	47
4. CONCLUSION .....	54
4.1. FUTURE WORKS .....	55
APPENDICES	
A. Spent fuel composition for LEU fuel after shutdown cooling for 10 years ....	57
B. Reactor core specifications.....	63
C. Isotopic composition for clad, structural, control rod, core barrel and reactor vessel.....	66
D. Three batch refueling arrangement for UOX-1/21-2.35/16-3.4/52-4.45 and UOX-2/09-2.35/32-3.4/48-4.45.....	70
E. Three batch refueling arrangement for MOX-1/RG/25-4.5/40-4.2/ 24-MOX and MOX-2/WG/25-4.5/40-4.2/ 24-MOX core.....	72
F. Three batch refueling arrangement for TRU-1/ 25-4.5/40-4.2/ 24-TRU core.....	74
BIBILOGRAPHY .....	76
VITA .....	78

## LIST OF FIGURES

Figure	Page
1.1. Isometric section view of SMR .....	3
2.1. A 11 x 11 robust fuel assembly for the SMR core .....	7
2.2. A standard layout of 17 x 17 fuel assembly.....	8
2.3. Core assembly layout for UOX-1/21-2.35/16-3.4/52-4.45 .....	11
2.4. Core assembly layout for UOX-2/09-2.35/32-3.4/48-4.45 .....	11
2.5. Pyrex rod configurations for UOX fuel .....	12
2.6. IFBA rod configurations for UOX fuel .....	12
2.7. MOX fuel assembly with 24 WABA pins .....	15
2.8. Core assembly layout for MOX-1/RG/25-4.5/40-4.2/24- MOX .....	16
2.9. Core assembly layout for MOX-2/WG/25-4.5/40-4.2/24- MOX .....	17
2.10. IFBA rod configurations for MOX fuel .....	17
2.11. Core assembly layout for TRU-1/25-4.5/40-4.2/24- TRU .....	19
2.12. A sample reflector core radial flux profile .....	23
3.1. 2D-radial neutron flux profile for UOX-1/21-2.35/16-3.4/52-4.45 .....	30
3.2. 2D-radial neutron flux profile for UOX-2/09-2.35/32-3.4/48-4.45 .....	30
3.3. The k-effective vs boron ( $B^{10}$ ) concentration for UOX fueled cores .....	34
3.4. Three batch refueling cycle for UOX-1/21-2.35/16-3.4/52-4.45 .....	35
3.5. Three batch refueling cycle for UOX-2/09-2.35/32-3.4/48-4.45 .....	35
3.6. 2D-radial neutron flux profile for MOX-1/RG/25-4.5/40-4.2 /24- MOX .....	39
3.7. 2D-radial neutron flux profile for MOX-2/WG/25-4.5/40-4.2 /24- MOX .....	40
3.8. The k-effective vs boron ( $B^{10}$ ) concentration for MOX fueled cores .....	42



3.9. Three batch refueling cycle for MOX-1 /RG/25-4.5/40-4.2/24- MOX .....	43
3.10. Three batch refueling cycle for MOX-2/WG/25-4.5/40-4.2/24- MOX .....	43
3.11. 2D-radial neutron flux profile for TRU-1/25-4.5/40-4.2/24- TRU .....	48
3.12. The k-effective vs boron ( $B^{10}$ ) concentration for TRU fueled core .....	50
3.13. Three batch refueling cycle for TRU-1/25-4.5/40-4.2/24- TRU .....	50

## LIST OF TABLES

Table	Page
1.1. List of light water SMRs around the world .....	4
2.1. Isotopic composition for UOX fuel .....	10
2.2. Isotopic composition for reactor grade MOX fuel .....	13
2.3. Isotopic composition for weapon grade MOX fuel .....	14
2.4. Isotopic composition for TRU fuel .....	19
2.5. SMR core properties .....	21
2.6. Average delayed neutron fraction for various fuel materials .....	24
2.7. Data entries for the BURN data card in MCNP .....	28
3.1. Reactor physics parameters for cores with LEU fuel arrangement .....	32
3.2. Total actinide composition for the UOX fueled cores .....	36
3.3. Decay heat values for the Pu vectors in the UOX spent fuel.....	38
3.4. Total non-actinide composition for the UOX fueled cores .....	38
3.5. Reactor physics parameters for cores with MOX fuel arrangement .....	41
3.6. Initial and final actinide composition for the reactor grade MOX fuel assembly.....	45
3.7. Initial and final actinide composition for the weapon grade MOX fuel assembly.....	45
3.8. Total non-actinide composition for the MOX fueled cores .....	46
3.9. Reactor physics parameters for cores with TRU fuel arrangement .....	49
3.10. Initial and final actinide composition for the TRU fuel assembly .....	51
3.11. Total non-actinide composition for the weapon grade TRU fueled core .....	52

## NOMENCLATURE

Symbol	Description
SMR	Small Modular Reactor
IRIS	International Reactor Innovative and Secure
NRC	Nuclear Regulatory Commission
LWR	Light Water Reactor
PWR	Pressurized Water Reactor
MCNP	Monte Carlo Neutron Particle
UOX	Uranium Oxide
LEU	Low Enriched Uranium
MOX	Mixed Oxide
TRU	Trans-Uranic
WABA	Wet Annular Burnable Absorber
IFBA	Integral Fuel Burnable Absorber
$k_{eff}$	Effective Multiplication Factor
$k_{prompt}$	Prompt Multiplication Factor
$\beta_{eff}$	Effective Delayed Neutron Fraction
SNF	Spent Nuclear Fuel
IAEA	International Atomic Energy Association
U	Uranium
Pu	Plutonium
Am	Americium
Cm	Curium

Np	Neptunium
Y	Yttrium
Zr	Zirconium
O	Oxygen
SYZ	Stabilized Ytria Zirconia
IMF	Inert Matrix Fuel
MA	Minor Actinides
RG	Reactor Grade
WG	Weapon Grade
RCCA	Rod Control Cluster Assembly
CASL	Consortium for Advanced Simulation of LWRs
VERA	Virtual Environment for Reactor Applications
RFA	Robust Fuel Assembly
MW	Megawatts

## 1. INTRODUCTION

Today most of the world's energy needs are supplied by oil (39.5 percent), coal (24.2. percent) and natural gas (22.1 percent) [1]. Although coal and oil are major energy producers, their attractiveness started to decline because of high greenhouse emission and large capital investment. Meanwhile, the demand for natural gas and nuclear power gradually began to rise. The advent of nuclear power in the early 1950s and 1960s was hailed as a reliable and a clean form of energy [1]. But post Chernobyl (26<sup>th</sup> April, 1986), Three Mile Island (25<sup>th</sup> March, 1979) and recent Fukushima Daiichi (11<sup>th</sup> March, 2011) accidents, the safety concerns surrounding the nuclear reactors questioned the future prospects of nuclear energy. In response, this also created an opportunity for the nuclear regulatory agencies around the globe to address the complex challenges associated with this technology and develop reactors which were consistent in terms of economy, reliability, safety, proliferation resistance and fuel and waste management.

Most of the commercial reactors operating around the world are large reactors with power output ranging between 1000 MWe and 1600 MWe. In general, such reactors provide a good voltage support for grid stability and also need a strong nuclear infrastructure with engineering capabilities in order to support it. Hence they are best suited only for the developed countries having large and well established electric grid systems [2]. However, the need to install reactors in countries with less power requirement, inadequate infrastructure or less established grid system have led to the concept of development of Small Modular Reactor (SMR)

## 1.1. SMALL MODULAR REACTORS

Small Modular Reactors are designed with a potential of providing clean and cost effective energy. As per the International Atomic Energy Association (IAEA) classification, SMRs are defined as reactors which produce power output of less than or equal to 300 MWe; but in general any reactor with an electrical output less than 700 MW is considered as a SMR. Based on the characteristics they are further categorized into three types 1) Light Water Reactors 2) High Temperature Gas Cooled Reactors and 3) Liquid Metal and Gas Cooled Reactors.

As shown in Figure 1.1, the scalability, modularity, robust design and enhanced safety features of the SMR offers great advantages over large commercial reactors

Modularity and flexibility: In contrast to large reactors, SMRs can be fabricated and assembled in a factory environment and then transported to the nuclear power site. This will help limit the on-site preparation and also reduce the lengthy construction duration further reducing the construction cost and making the SMRs 20 to 30 percent less expensive [4]. In addition, the scalability and flexibility features of SMR also makes it more suitable for small isolated areas with low energy demands, limited infrastructure and smaller and less established grid system.

Passive safety system: The integral design of SMR makes it safer in case of any severe accidents preventing any radiation leak into the environment. The passive safety system is another important safety feature in the SMR. In case of loss of coolant accident, this system shuts down the reactor and cools it without any human intervention or AC power for a period of seven days. The safety system incorporates an on-site water inventory which operates on natural forces (i.e. natural circulation or gravity or compressed gas) [5].

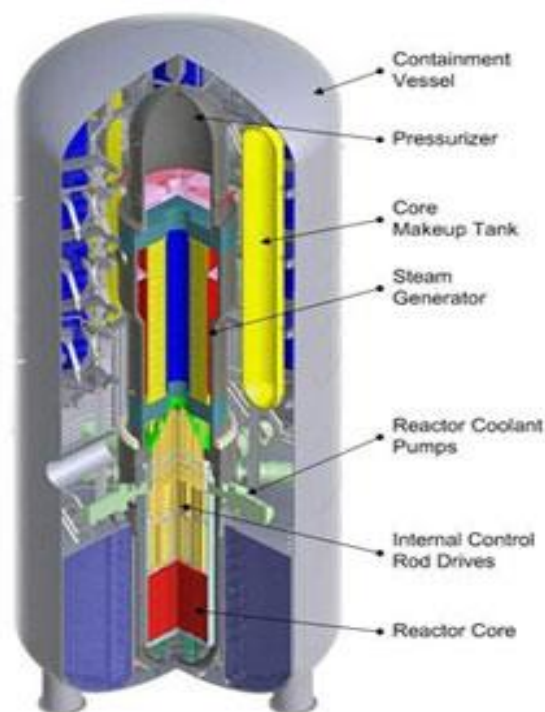


Figure 1.1. Isometric section view of SMR [3].

Non-proliferation resistant and security: The SMR is a sealed unit built below grade thus making it safer against any terrorist activities or aircraft impact or any vulnerabilities due to natural phenomenon. They are also designed to operate for longer periods without refueling (i.e. approximately 18 to 24 months); and the reactor can be refueled in a factory environment and then transported back to site thus securing it against any proliferation issues.

## 1.2. CURRENT STATUS OF SMR IN USA

At present researches are carried out on SMRs for all principal reactor types (i.e. Light Water Reactors (LWR), Heavy Water Reactors (HWR) and Gas Cooled Reactors (GCR)) [6]. Table 1.1 shows the list of light water SMRs that are under development

around the world. Each of these reactors listed in the table are differentiated based on their design, safety features, power output, operating conditions and fuel characteristics.

Table 1.1. List of light water SMRs around the world [6].

Country	Reactor Name	Power Output (MWt)	Operating Conditions, P (MPa) / T (°C)	Fuel Type / Enrichment
	Westinghouse	800	15.5 / 310	UO <sub>2</sub> / < 5%
USA	NuScale	165	12.8 / -	UO <sub>2</sub> / < 4.95%
	mPower	500	14.1 / 320	UO <sub>2</sub> / 5%
IRIS	-	1000	15.5 / 330	UO <sub>2</sub> -MOX / 4.95%
Russia	WWER	850	16.2 / 325	UO <sub>2</sub> / 4.95%
	KLT-30S	150	12.7 / 316	UO <sub>2</sub> / < 20%
Japan	IMR	1000	15.5 / 345	UO <sub>2</sub> / 4.8%
China	CNP-300	999	15.2 / 302	UO <sub>2</sub> / 2.4 - 3%
Argentina	CAREM	100	12.25 / 326	UO <sub>2</sub> / 3.1%

Some of the major ongoing projects in recent years in the USA are briefly detailed below.

NuScale: The NuScale SMR is an integral pressurized LWR consisting of 12 independent modules each capable of producing an output of 45 MWe. The preliminary designs for the SMR are in accordance with the Multi Application Small Light Water Reactor (i.e. MASLWR), which was developed in 2003 by the Oregon State University in collaboration



with the Idaho National Engineering Lab and the Nexant Bechtel [3]. The reactor is built below grade and includes advanced safety features like the passive decay heat removal and containment heat removal systems [6]. Furthermore the reactor is sealed in a high pressure containment vessel which is submerged completely in water in a safety related pool thus providing safety benefits in case of radiation leaks. The plant is designed to operate for 24 months without refueling, and has a design life of 60 years. In addition it is also capable of accommodating the used nuclear fuel for all the 12 modules just like the large commercial reactors [6].

B&W mPower: The mPower is again an integral PWR single unit designed by Babcock and Wilcox (B&W) with a capacity of 150 MWe. The reactor is built below grade with an operating cycle of 48 months without refueling and has a design life of 60 years. The core consists of total 69 fuel assemblies without any soluble boron in the reactor coolant to control the reactivity. In addition to having the same design and safety features as that of NuScale SMR, the mPower is also designed with a low core linear heat rate which reduces the fuel and clad temperatures in case of an accident and a large coolant volume system which provides a timely safety response in case of loss of coolant accidents (LOCA) [6].

Westinghouse SMR: Westinghouse SMR is again a single unit PWR capable of producing an electrical output of 200 MW. The core is a partial version of AP1000 core consisting of total 89 fuel assemblies with an active core height of 2.4 meters. The passive safety feature cools the reactor during accident without any human intervention or external pumps for a period of seven days. The cooling is carried out due to natural forces (i.e. gravity or natural circulation or compressed gas).

### 1.3. RESEARCH OBJECTIVES

The main objective of this research was to first model a reference reactor based on the Westinghouse light water SMR with low enriched uranium (LEU) fuel using the MCNP code. This was done by determining the radial thermal flux distribution profile and also the important reactor physics parameters like the delayed neutron fraction, the control rod worth and the reactivity co-efficient at the beginning of life (BOL) and comparing it with a standard UO<sub>2</sub> based PWR. Furthermore, the equilibrium cycle was also determined and analyzed for its spent fuel composition. Using this referenced core and following the same procedure, the SMR was then analyzed for mixed-oxide (MOX) and transuranic (TRU) fueled cores in order to predict its behavior with flexible fuel configurations.

## 2. CORE MODEL AND METHODOLOGY

Details about the reactor core design is presented in this section. The core geometry and the fuel assembly configurations are modelled in accordance with the Westinghouse's SMR. Furthermore, the fuel enrichment strategies and its arrangement in order to keep the reactor critical are also discussed. Finally, the methodology and the reactor operating conditions for the simulation of the model are also detailed in this section.

### 2.1. CORE GEOMETRY

The core used for the analysis was a Westinghouse's SMR, an integral PWR with an active core height of 2.4 meter (~8 feet). Figure 2.1 shows the cross sectional view of the assembly layout for the SMR core also indicating the location of the control rod drive mechanisms.

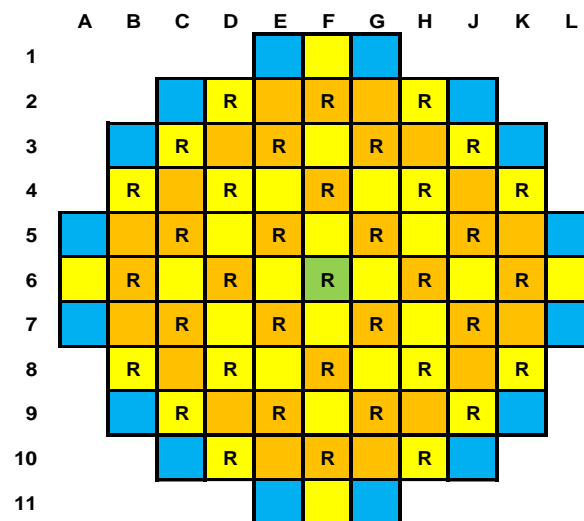


Figure 2.1. A 11 x 11 robust fuel assembly for the SMR core [7].

The core consists of a 11 x 11 robust fuel assembly (RFA) design with a total of 89 assemblies (i.e. 52 fuel assemblies and 37 control rod drive mechanisms) contained within a core barrel and reactor vessel itself. The reactor vessel components were based on AP1000 design but modified to a reduced dimensions of 3.5 meter diameter and 24.7 meter height [6].

## 2.2. FUEL ASSEMBLY CONFIGURATIONS

The fuels investigated for the study were uranium-oxide (UOX) fuel (i.e. with less than 5%  $U^{235}$  enrichment), mixed-oxide (MOX) fuel (i.e. with reactor and weapon grade plutonium) and transuranic (TRU) fuel (i.e. with actinides from the spent fuel composition of UOX fuel). The fuel assembly (Figure 2.2) was a square lattice, a standard 17 x 17 layout with 264 fuel rod locations, 24 guide tube locations and 1 central location for instrumentation, incorporating the standard Westinghouse design specifications.

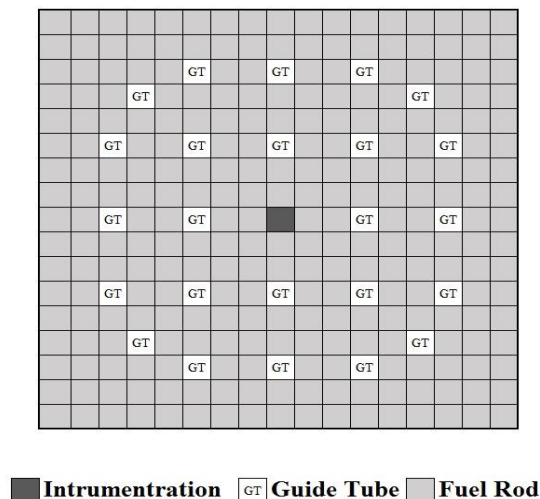


Figure 2.2. A standard layout of 17 x 17 fuel assembly [8].

The fuel rod consisted of a uniform cylindrical pellet stacked together within a Zircaloy clad tube. Between the fuel stack and the clad, a clearance was provided in order to accommodate the fuel swelling due to accumulation of fission products thereby preventing clad rupture. The gap was filled with helium gas to improve heat conduction from fuel to cladding. The guide tubes in the fuel assembly served as a location for the insertion of Rod Cluster Control Assembly (RCCA). The RCCA is a spider assembly consisting of evenly spaced control rods that is either Silver Indium Cadmium or Boron Carbide rods based on the type of fuel used. Detailed specifications for the fuel rod, the clad, the structural, the control rod and the burnable poison (i.e. discrete and integral) were taken from CASL (Consortium for Advanced Simulation of LWRs) VERA core physics benchmark specifications [8] and are presented in Appendix B. The isotopic compositions for the standard materials like the clad, the control rods, the burnable poisons, the core barrel and the reactor vessel are presented in Appendix C.

**2.2.1. Uranium-oxide Fuel Assembly.** The UOX fuel used was a low enriched uranium (LEU) fuel with less than 5%  $U^{235}$  enrichment and density of  $10.36 \text{ g/cm}^3$  (i.e. 95% of theoretical density). The core loading pattern involved the radial placement of the fuel assemblies as well as the burnable poisons. There were three regions of fuel assemblies with the central and the intermediate regions of the core loaded with 2.35w/o and 3.4w/o  $U^{235}$  fuel whereas the outer peripheral region was loaded with 4.45w/o  $U^{235}$  fuel. This type of loading pattern with varying enrichment permitted a flatter radial power profile and helped establish a favorable power distribution in the core.

For the analysis, only  $U^{235}$  and  $U^{238}$  isotopes were taken into consideration and the composition for these isotopes for each of the enrichment were determined as shown in Table 2.1.

Table 2.1. Isotopic composition for UOX fuel

Nuclide	w/o (2.5)	w/o (3.4)	w/o (4.5)	Remarks
U <sup>235</sup>	2.071	2.997	3.922	
U <sup>238</sup>	86.076	85.150	84.225	$\rho = 10.36 \text{ g/cc}$
O <sup>16</sup>	11.853	11.853	11.853	

Figures 2.3 and 2.4 shows the fuel assembly loading pattern for the LEU cores. The two cores are different in terms of the amount of enrichment which also corresponds to the amount of fissile (i.e. U<sup>235</sup>) material, the fuel arrangement strategies and burnable poison configurations. The core UOX-1 consists of 21 nos. of 2.35w/o U<sup>235</sup>, 16 nos. 3.4w/o U<sup>235</sup> and 52 nos. 4.45 w/o U<sup>235</sup> fuel assemblies with 1160.001 kgs of fissile material whereas the core UOX-2 consists of 09 nos. of 2.35w/o U<sup>235</sup>, 32 nos. 3.4w/o U<sup>235</sup> and 48 nos. 4.45 w/o U<sup>235</sup> fuel assemblies with 1190.93 kgs of fissile material.

The excess reactivity in the core during the fuel cycle were partially controlled using the Discrete Burnable Absorbers (PYREX) and Integral Fuel Burnable Absorbers (IFBA). The PYREX rod used was a borosilicate (B<sub>2</sub>O<sub>3</sub> – SiO<sub>2</sub> with 12.5w/o B<sub>2</sub>O<sub>3</sub>) glass tube enclosed within a stainless steel (SS 304) clad with B<sup>10</sup> (i.e. a neutron absorber) loading of 6.535 mg/cm whereas IFBA was a ZrB<sub>2</sub> coating over fuel rods with B<sup>10</sup> loading of 2.355 mg.

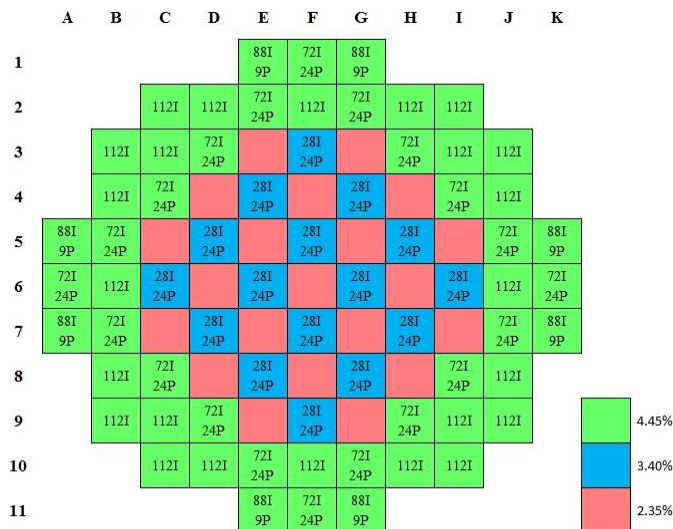


Figure 2.3. Core assembly layout for UOX-1/21-2.35/16-3.4/52-4.45.

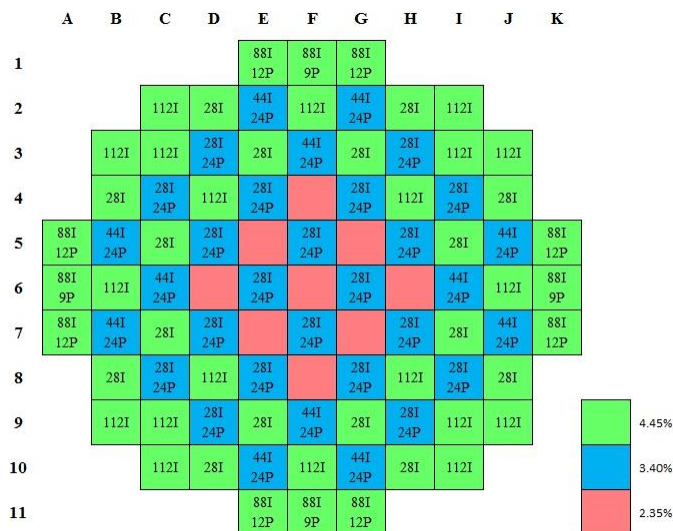


Figure 2.4. Core assembly layout for UOX-2/09-2.35/32-3.4/48-4.45.

The PYREX rod and IFBA arrangement are shown in Figures 2.5 and 2.6. The placement of the assemblies containing these burnable absorbers within the core are also shown in Figures 2.3 and 2.4.

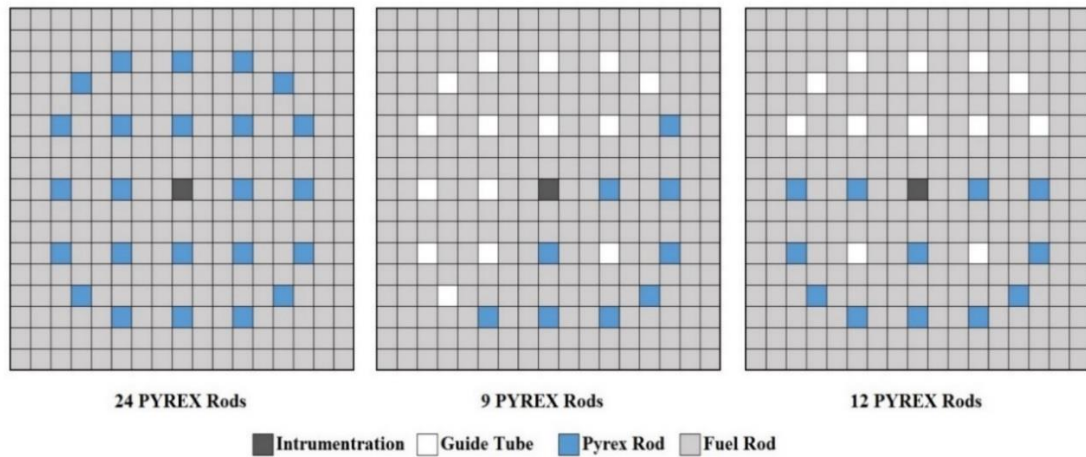


Figure 2.5. Pyrex rod configurations for UOX fuel [9].

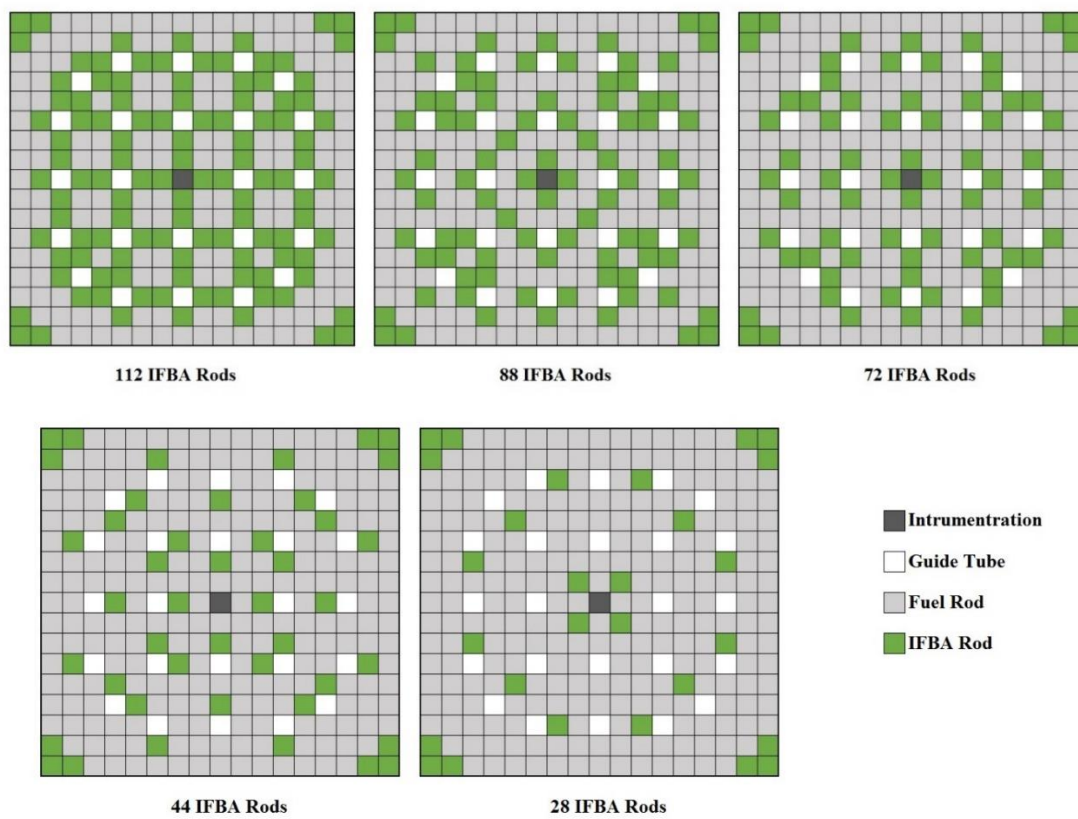


Figure 2.6. IFBA rod configurations for UOX fuel [9].



The burnable poisons helped in limiting the peaking factor and prevent any positive temperature reactivity co-efficient under normal reactor operating conditions. Furthermore, the boron in each of these poisons got depleted completely at the end of cycle thus preventing any residual reactivity within the core.

Control rods are another important component of the reactor that are used to adjust the reactivity of the core. They are designed for coarse control, fine control or complete shut-down of the reactor core. The materials for control rods are selected based on its absorption cross section for neutrons and lifetime as an absorber. Only black rods were considered; the ones which absorb all the incident neutrons. The control rod material selected for LEU fuel was a Ag-In-Cd rod with 80% Ag, 15% In and 5% Cd and with a poison density of 10.2 g/cm<sup>3</sup>.

**2.2.2. Mixed-oxide Fuel Assembly.** Mixed oxide fuel is a nuclear fuel which contains more than one oxide of fissile material (i.e. plutonium blended with natural uranium or reprocessed uranium or depleted uranium; PuO<sub>2</sub> + UO<sub>2</sub>). Here, MOX fuel with weapon grade plutonium (WG) as well as reactor grade (RG) plutonium blended with depleted uranium (i.e. 0.25w/o U<sup>235</sup>) was considered. Tables 2.2 and 2.3 indicates the isotopic composition of MOX fuel with RG and WG plutonium.

Table 2.2. Isotopic composition for reactor grade MOX fuel.

Nuclide	w/o (4.2)	w/o (4.5)	Remarks
U <sup>235</sup>	3.702	3.966	ρ = 10.36 g/cc
U <sup>238</sup>	84.445	84.181	
O <sup>16</sup>	11.853	11.853	

Table 2.2. Isotopic composition for reactor grade MOX fuel (cont.)

Nuclide	w/o (2.5)	w/o (3)	w/o (4)	
U <sup>235</sup>	0.172	0.171	0.168	
U <sup>238</sup>	85.775	85.335	84.015	
Pu <sup>238</sup>	0.044	0.053	0.079	$\rho = 10.36 \text{ g/cc};$
Pu <sup>239</sup>	1.299	1.559	2.339	Reactor Grade Plutonium Composition:
Pu <sup>240</sup>	0.528	0.634	0.952	Pu <sup>238</sup> = 2%,
Pu <sup>241</sup>	0.242	0.291	0.432	Pu <sup>239</sup> = 53%,
Pu <sup>242</sup>	0.110	0.132	0.198	Pu <sup>240</sup> = 24%,
O <sup>16</sup>	11.828	11.824	11.815	Pu <sup>241</sup> = 15%, Pu <sup>242</sup> = 6%

Table 2.3. Isotopic composition for weapon grade MOX fuel.

Nuclide	w/o (2.5)	w/o (3)	w/o (4)	Remarks
U <sup>235</sup>	0.172	0.171	0.168	$\rho = 10.36 \text{ g/cc};$
U <sup>238</sup>	85.775	85.335	84.015	Weapon Grade Plutonium Composition:
Pu <sup>238</sup>	0	0	0	Pu <sup>238</sup> = 0%,
Pu <sup>239</sup>	2.064	2.477	3.715	Pu <sup>239</sup> = 93.6%,
Pu <sup>240</sup>	0.130	0.156	0.234	Pu <sup>240</sup> = 5.9%,
Pu <sup>241</sup>	0.0088	0.01106	0.0158	Pu <sup>241</sup> = 0.4%,
Pu <sup>242</sup>	0.0022	0.0026	0.0039	Pu <sup>242</sup> = 0.1%
O <sup>16</sup>	11.848	11.752	11.846	

From Figure 2.7, it can be observed that the MOX assembly consisted of two regions of fuel assemblies where the central region was loaded with 4.5% of MOX fuel and the surrounding outer region loaded with 2.5% and 3% of MOX fuel respectively. The excess reactivity was controlled by using Wet Annular Burnable Absorbers (WABA) in lieu of PYREX rods. The IFBA rods were not considered in the MOX assembly because of the restrictions placed by the Department of Energy (DOE) due to lack of burnup experience for such configurations. WABA is a discrete burnable absorber with annular pellets of  $\text{Al}_2\text{O}_3 - \text{B}_4\text{C}$  (i.e. with 14w/o  $\text{B}_4\text{C}$ ) and wet water filled central region. Its annularity provides benefits over other burnable poison in terms of increased neutron moderation, reduced neutron absorption and better absorber depletion. The WABA used in the MOX assembly was loaded with 6.165 mg/cm of  $\text{B}^{10}$  and inserted in the guide tubes.

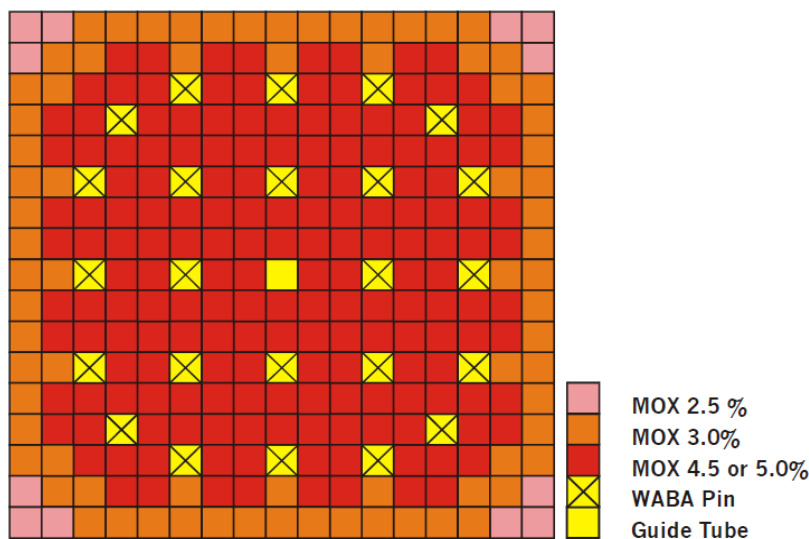


Figure 2.7. MOX fuel assembly with 24 WABA pins [10].

The core loading pattern was based on the following assumptions:

1. No MOX assembly was placed adjacent to each other.
2. No MOX assembly in the control rod position.
3. Maximum 1/3<sup>rd</sup> (i.e. 30%) of the core was loaded with MOX assembly.
4. No MOX assembly on the outer periphery of the core.
5. IFBA was used only for the UO<sub>2</sub> fuel assemblies.
6. No Minor Actinide (i.e. Am-Americium) was used in the MOX fuel assembly.

Based on these guidelines, cores with RG and WG plutonium were modelled as shown in Figures 2.8 and 2.9.

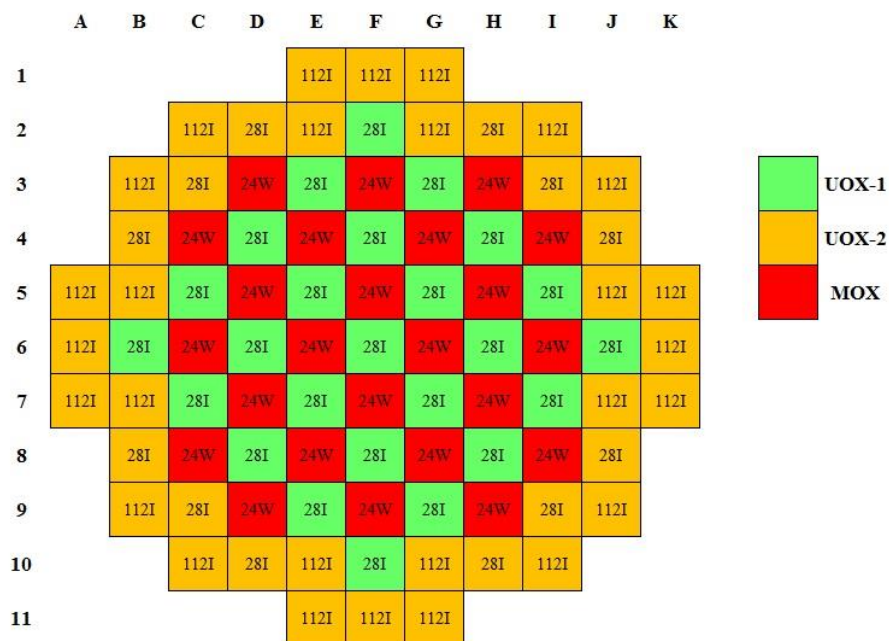


Figure 2.8. Core assembly layout for MOX-1/RG/25-4.5/40-4.2/24- MOX.

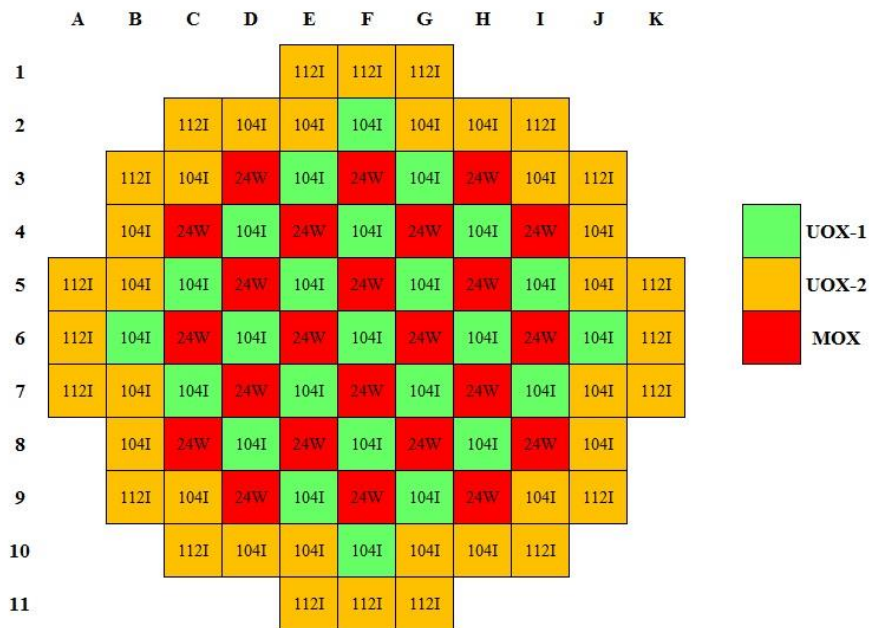


Figure 2.9. Core assembly layout for MOX-2/WG/25-4.5/40-4.2/24- MOX.

The IFBA arrangements for the UO<sub>2</sub> fuel assemblies used in the cores are shown in Figure 2.10.

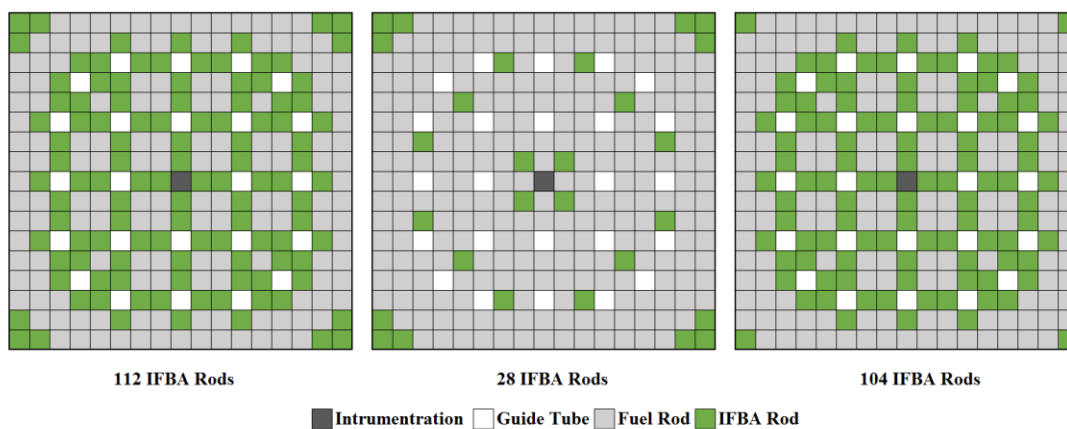


Figure 2.10. IFBA rods configuration for MOX fuel [10].

The two cores differ from each other in terms of its poison configuration and the type of plutonium used for the MOX fuel assembly. The core MOX-1 consists of 25 nos. 4.5w/o  $U^{235}$ , 40nos. 4.2w/o  $U^{235}$  and 24 nos. reactor grade MOX fuel assemblies with 1342.449 kgs of fissile material. The core MOX-3 consists of 25 nos. 4.5w/o  $U^{235}$ , 40nos. 4.2w/o  $U^{235}$  and 24 nos. weapon grade MOX fuel assemblies with 1340.340 kgs of fissile material

Again only black control rods were considered for the analysis. The control rod material selected for MOX fuel was a Boron Carbide ( $B_4C$ ) rod with maximum 20% carbon and minimum 80% boron composition and with a poison density of  $2.016 \text{ g/cm}^3$ . Detailed specification for the control rods are provided in Appendix B.

**2.2.3. Tran-uranic Fuel Assembly.** A similar approach to that of the MOX core was adopted in defining the TRU fuel assembly. A heterogeneous mode of loading pattern was followed wherein radionuclides to be transmuted were recycled and separated from the standard fuel and placed at specific locations within the core. Figure 2.11 shows a layout of TRU fuel assembly with its central region loaded with 24 nos. TRU fuel and 25 nos. 4.5w/o  $U^{235}$  fuel and surrounded by 40 nos. 4.2 w/o  $U^{235}$  fuel in its outer periphery.

In thermal reactors, the transmutation of radionuclides leads to increased neutron generation due to its low neutron fission to capture ratio. To overcome this positive neutron population and also to partially control the excess reactivity discrete burnable absorbers (i.e. WABA) and IFBA rods were again used in the fuel assemblies. The poison configurations used were similar to those for MOX and LEU cores.

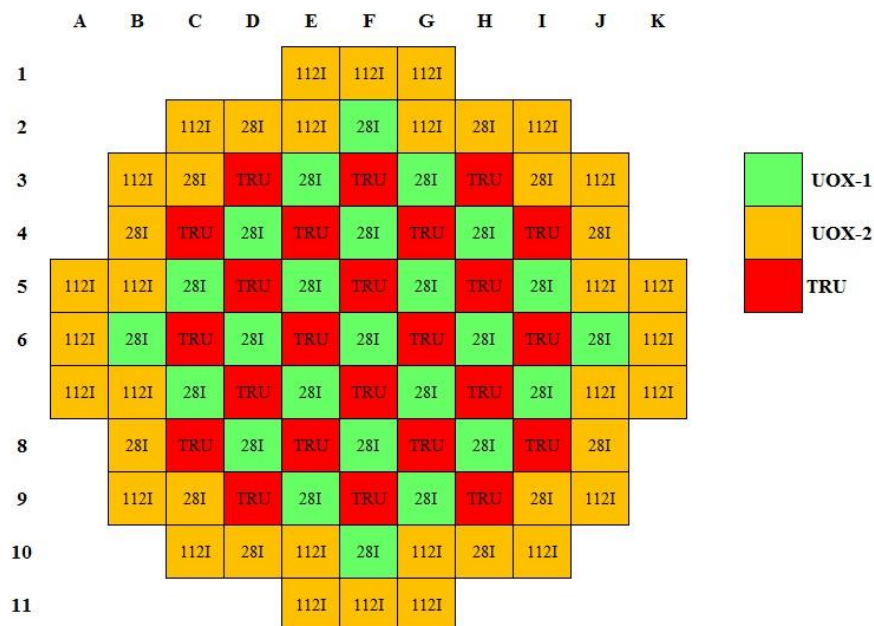


Figure 2.11. Core assembly layout for TRU-1/25-4.5/40-4.2/24- TRU.

Transuranic fuels were characterized by high concentration of plutonium (Pu) content and low concentration of minor actinides (i.e. Np, Am and Cm) content as shown in Table 2.4 which specifies the isotopic composition of the fuel pin. The minor actinide composition in the fuel pin was determined from after shut-down cooling of spent fuel of UOX core for a period of 10 years as shown in Appendix A.

Table 2.4. Isotopic composition for TRU fuel.

Nuclide	Weight Percent (w/o)	Remarks
Np <sup>237</sup>	0.3701	ρ = 10.3169 g/cc;
Pu <sup>238</sup>	0.1053	
Pu <sup>239</sup>	4.8212	

Table 2.4. Isotopic composition for TRU fuel (cont.)

Pu <sup>240</sup>	1.5074	Fuel (8w/o - TRU) + Inert Matrix (92w/o - YSZ).
Pu <sup>241</sup>	0.5124	
Pu <sup>242</sup>	0.2754	
Am <sup>241</sup>	0.3543	YSZ : 64.696w/o Y <sub>2</sub> O <sub>3</sub> and 35.304w/o ZrO <sub>2</sub>
Am <sup>242</sup>	0.0002	
Am <sup>243</sup>	0.0463	
Cm <sup>242</sup>	0.00000063	
Cm <sup>243</sup>	0.0001	
Cm <sup>244</sup>	0.0067	
Cm <sup>245</sup>	0.0004	
Cm <sup>246</sup>	0.000032	
Y <sup>89</sup>	30.6910	
Zr <sup>90</sup>	15.7905	
Zr <sup>91</sup>	3.4435	
Zr <sup>92</sup>	5.2635	
Zr <sup>94</sup>	5.3341	
Zr <sup>96</sup>	0.8593	
O <sup>16</sup>	30.6180	

Since the fissile isotope content of plutonium and actinides were higher in TRU fuels so an inert non fissile matrix was required to support the fuel structure. This was achieved either by adopting a homogeneous solution phase (i.e. solid or liquid) or a heterogeneous composite phase (i.e. fissile material + inert matrix). The TRU fuel pin used was a composite mixture of 8w/o fissile material (i.e. TRU fuel) and 92w/o inert matrix (i.e. Yttrium Stabilized ZrO<sub>2</sub> matrix –YSZ). Due to YSZ's high insolubility and durability, it was selected over ZrO<sub>2</sub>/MgO matrix. The control rod specification were similar to those used in MOX core.



### 2.3. NEUTRON TRANSPORT CALCULATIONS

All the fuel assemblies were modelled using Monte Carlo Neutron Particle (MCNPX\_2.7.0) code. The cross section for all materials (i.e. fuel, clad, moderator and structural) were taken from ENDF/B-VII libraries at 600K temperature. Table 2.5 specifies the core properties and the operating conditions used for the simulation of the model.

Table 2.5. SMR core properties.

Details	Units	Value
Reactor Thermal Power	MWt	900
Operating Temperature	K	600
Operating Pressure	Bar	155
Moderator Density	g/cm <sup>3</sup>	0.661
Assemblies	Nos.	89
Pitch to Diameter Ratio	Cm	1.258

The study was carried out by first referencing the SMR core with the LEU fuel. This was done by determining the reactor physics parameters like the 2-D radial thermal flux profile, the average to maximum flux ratio, the effective multiplication factor, the delayed neutron fraction, the control rod worth or the shutdown margin at normal operating conditions and at cold shut-down conditions, the critical boron concentration and the reactivity co-efficient at the beginning of life (BOL). Once the LEU core was referenced, it was then analyzed for MOX and TRU fuels respectively using the same procedure. Furthermore, the equilibrium cycle for each of these oxide fueled cores was also

determined and the spent nuclear fuel was analyzed for important radionuclides for its composition and decay heat.

## 2.4. NEUTRONIC METHODOLOGY

**2.4.1. Radial Neutron Flux Profile.** The neutron balance within the reactor core is because of neutron production due to fission and neutron losses due to absorption and leakage. The rate of change of neutron flux for thermal reactor is given by the following equation

$$\frac{d\phi}{dt} = \Sigma_s \phi - \Sigma_a \phi - \text{Leakage Divergence} \quad (1)$$

where  $\Sigma_s \phi$  = scattering reaction rate of fast neutrons i.e. source term ( $n/cm^2$ ),

$\Sigma_a \phi$  = neutron absorption rate i.e. loss term ( $n/cm^2$ )

The leakage divergence is the result of neutron tendency to diffuse from the high concentrations region (i.e. the core center) to the low concentrations region (i.e. the outer periphery of the core). The leakage is minimized by the use of reflector condition (i.e. light water), the purpose of which is to only thermalizes the fast moving neutrons [11]. Figure 2.12 shows the sample radial neutron flux profile for reactor cores with reflectors.

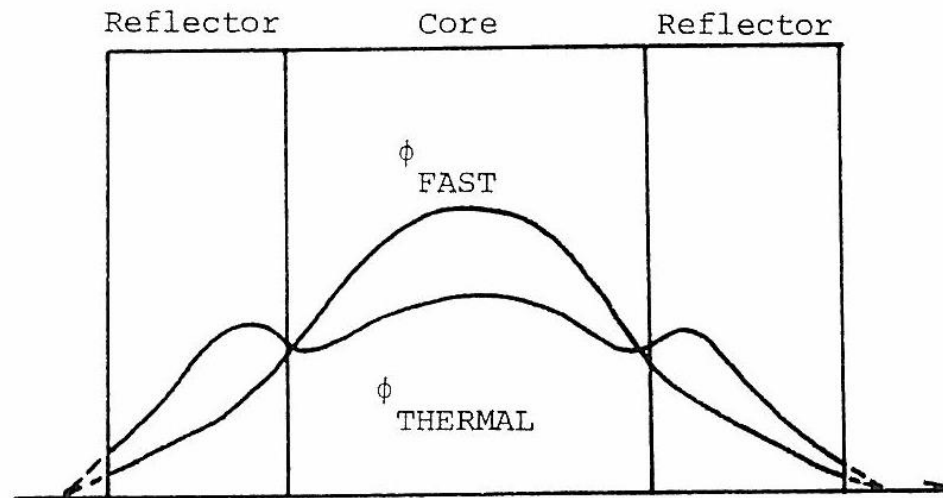


Figure 2.12. A sample reflector core radial flux profile [11].

This is the behavior is expected for the radial neutron flux profiles for each of the cores. The flux values for these cores are determined using the FMESH tally in the MCNPX simulation. For this purpose, a rectangular mesh was superimposed over the core cross section in the x and y direction and averaged over the core height along the z direction, using the KCODE calculations. The flux values obtained were then plotted using the MATLAB software to obtain the 2-D radial thermal flux profile map and also determine the maximum to average flux ratio.

**2.4.2. Delayed Neutron Fraction.** The presence of delayed neutrons plays a significant role in reactor control due to its impact on reactor power change rate. Table 2.6 provides the standard delayed neutron fraction values for common fuel materials.

Table 2.6. Average delayed neutron fraction for various fuel materials [12].

Group	Half Life (sec)	Uranium-235	Uranium-238	Plutonium-239
1	55.6	0.00021	0.0002	0.00021
2	22.7	0.00141	0.0022	0.00182
3	6.22	0.00127	0.0025	0.00129
4	2.30	0.00255	0.0061	0.00199
5	0.61	0.00074	0.0035	0.00052
6	0.23	0.00027	0.0012	0.00027
Average		0.00650	0.0157	0.0020

The delayed neutron fraction for each of the cores was calculated by using MCNP. First the effective multiplication factor was determined by inserting the KCODE data card which implies the use of prompt as well as delayed neutrons for criticality calculations. Then using the TOTNU data card with an entry NO, the prompt neutron multiplication factor was calculated. The 'TOTNU NO' prevents any influence due to delayed neutrons in the criticality calculations. Based on the values obtained the effective delayed neutron fraction was determined using equation 2.

$$\beta_{eff} = 1 - \frac{k_p}{k_{eff}} \quad (2)$$

where  $\beta_{eff}$  = Effective Delayed Neutron Fraction,

$k_p$  = Prompt Neutron Multiplication Factor,

$k_{eff}$  = Effective Neutron Multiplication Factor.

The prompt neutron generation time as a function of delayed neutron fraction can be calculated using the following equation.

$$T_{\text{average}} = T_{\text{prompt}} (1-\beta) + T_{\text{delayed}} \beta \quad (3)$$

where  $T_{\text{prompt}}$  = Prompt Neutron Generation Time (seconds)

$T_{\text{delayed}}$  = Delayed Neutron Generation Time (seconds)

**2.4.3. Control Rod.** Control rods are used to compensate the excess reactivity in the reactor core by inserting large amount of negative reactivity. Their purpose is not limited to reactivity control alone but also used in adjusting the reactor power level or shutdown the reactor during accident or refueling. The control rod worth was calculated by determining the multiplication factor when all the control rods are completely inserted and when all the control rods are completely withdrawn using MCNP and inserting them in the following equation 3.

$$\Delta\rho = \frac{k_{in} - k_{out}}{k_{in}k_{out}} \quad (4)$$

where  $\Delta\rho$  = Control rod worth (Dollars),

$k_{out}$  = Effective multiplication factor with all control rod completely withdrawn,

$k_{in}$  = Effective multiplication factor with all control rod completely inserted

Another important feature of the control rod is its ability to scram the reactor during cold operating conditions (i.e. cold shut-down condition). The approach adopted was similar but now with material cross sections considered at 300K temperature.

**2.4.4. Temperature Reactivity Co-efficient.** Temperature reactivity co-efficient are another important safety feature in reactor design which signifies change in reactivity per degree change in temperature. Usually the two dominant temperature reactivity

coefficients are moderator temperature co-efficient (i.e. delayed temperature co-efficient) and fuel temperature coefficient (i.e. prompt temperature co-efficient). Generally from a safety point of view all reactors are designed with negative temperature reactivity co-efficient. The negative sign indicates that for an abrupt change in the power or excess positive reactivity insertion there would be sufficient negative feedback in the reactor which would keep it subcritical and prevent any damage to the reactor core.

$$\Delta\rho_f = \frac{k_2 - k_1}{k_1} \quad (5)$$

$$\Delta\rho_{fm} = \frac{k_3 - k_1}{k_1} \quad (6)$$

$$\Delta\rho_m = \Delta\rho_{fm} - \Delta\rho_f \quad (7)$$

$$\frac{\delta k_f}{^\circ\text{C}} = \frac{\Delta\rho_f}{\Delta T} \quad (8)$$

$$\frac{\delta k_m}{^\circ\text{C}} = \frac{\Delta\rho_m}{\Delta T} \quad (9)$$

where  $\Delta\rho_f$  = Reactivity change for fuel

$\Delta\rho_{fm}$  = Reactivity change for fuel and moderator

$\Delta\rho_m$  = Reactivity change for moderator

$k_1$  = Multiplication factor with fuel and moderator at base temperature

$k_2$  = Multiplication factor with fuel at increment temperature

$k_3$  = Multiplication factor with fuel and moderator at increment temperature

$\Delta T$  = Temperature difference ( $^\circ\text{C}$ )

$\frac{\delta k_f}{^\circ\text{C}}$  = Co-efficient of reactivity for fuel

$\frac{\delta k_m}{^\circ\text{C}}$  = Co-efficient of reactivity for moderator

The temperature reactivity co-efficient for fuel and moderator were calculated by using the above equations. The  $k_{\text{eff}}$  values for fuel and moderator were obtained using MCNP at base temperature of 600K and for increment temperature of 900K respectively.

**2.4.5. Critical Boron Concentration.** Another method commonly used in controlling the excess reactivity is the chemical shim which includes introduction of boric acid ( $\text{H}_3\text{BO}_3$ ) in the reactor coolant. Controlled use of boron concentration in the coolant helps achieve optimum fuel assembly poisoning and also compensates for reactivity changes due to major coolant temperature changes between cold shut-down and full power operation. But care also needs to be taken to limit excess use of chemical shim in order to avoid any effects due to increase in coolant temperature which will reduce the shim's reactivity effects thereby resulting in positive moderator temperature co-efficient, a major safety drawback and also due to its slow removal rate.

The critical boron concentration was calculated by determining the  $k_{\text{eff}}$  values using MCNP code for varying boron concentrations in the reactor coolant. The values obtained were then plotted using the EXCEL software and the boron concentration in ppm (parts per million) for the  $k_{\text{eff}}$  equal to 1 (i.e. critical condition) was determined.

**2.4.6. Burn-up Calculations.** The main objectives of the burn up calculations for the study were:

1. To determine the variations in the radial thermal flux distribution with the operation time.
2. To determine the equilibrium cycle.
3. To analyze the spent fuel composition in terms of mass for important fission products (i.e. actinides and non-actinides).

The burn up calculations were done using MCNPX with the help of the BURN data card. Following Table 2.7 indicates the entries used within the BURN card.

Table 2.7. Data entries for the BURN data card in MCNP [13].

Data Card	Value	Details
POWER	900	The thermal reactor operating power in MWt
TIME	-	The reactor operating time in days for each burn cycle. Generally small increment time steps of less than 100 days were set for accurate results.
PFRAC	1.0	The power fraction which was set at 1.0 indicating a steady power throughout the operation cycle.
MAT	-	The materials to be burned (i.e. Fuel rods, PYREX rods and IFBA rods).
MATVOL	-	The corresponding total volume of the materials to be burned.
OMIT	-	The isotopes omitted in the burn calculations lacking the cross section tables.
BOPT = b <sub>1</sub> b <sub>2</sub>	b <sub>1</sub> = 1.0	Q – value multiplier.
	b <sub>2</sub> = -14	The b <sub>2</sub> value used indicates that the burn output will include the 2-tier fission products arranged based on increasing ZZZAAA displayed at the end of each time step.



**2.4.6.1. Refueling strategy.** The refueling process in a PWR is tedious as well as time consuming. The process involves the transfer of the entire core assembly to the spent pool where each of the assemblies are inspected thoroughly and then based on the amount of fissile material, the most depleted fuel assemblies are replaced with fresh ones. Here, this was achieved by following a three batch refueling approach with an expected operating cycle of 12 to 24 months as shown in Appendix D, E and F. In each batch refueling technique, 1/3<sup>rd</sup> of the core (i.e. 36 fuel assemblies) was replaced with a set of fresh fuel assemblies and its central assembly been replaced always in each of the burn cycle.

**2.4.6.2. Equilibrium cycle and nuclear spent fuel.** “Equilibrium cycle refers to the fuel cycles that occur after one or two initial cycles of reactor operation having similar fuel characteristics”[14]. Here, the equilibrium cycle was obtained after two initial burn cycles. Based on the output from the burn calculations, the effective multiplication factor against the reactor operating time for each of the cores were plotted using the EXCEL plotting software. In addition the spent fuel composition of the equilibrium cycle for important actinides and non-actinides were also analyzed.

### 3. RESULTS AND DISCUSSION

#### 3.1. URANIUM-OXIDE FUEL

Radial neutron flux profile: Figures 3.1 and 3.2 shows the 2 dimensional radial neutron flux map for the UOX fueled cores.

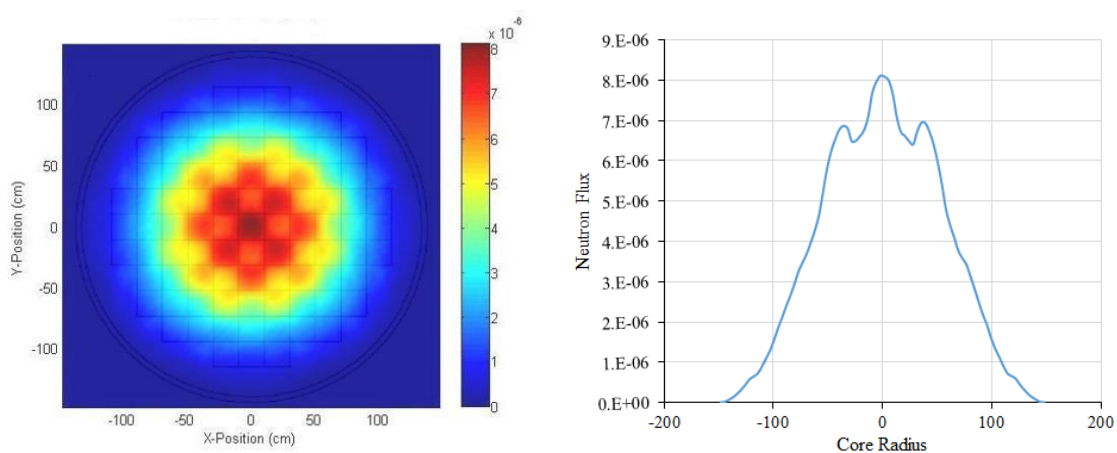


Figure 3.1. 2D-radial neutron flux profile for UOX-1/21-2.35/16-3.4/52-4.45.

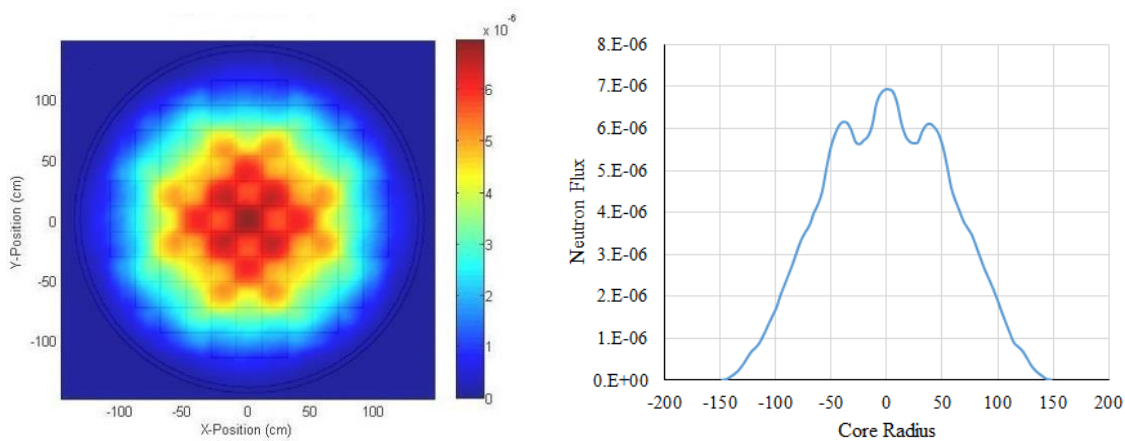


Figure 3.2. 2D-radial neutron flux profile for UOX-2/09-2.35/32-3.4/48-4.45.

It can be observed from the figures, that in both the cases the flux profile is uniformly distributed throughout the core. This even distribution is due to the uniform loading of the fuel and the burnable absorber, which ensures predictable core temperatures and uniform fuel depletion during the reactor operation. The maximum neutron flux at the central fuel assembly indicates a high source of heat generation in that region. From the figures, higher flux was also observed in the region surrounding the central assembly particularly in 2.35 enriched  $\text{UO}_2$  fuel assemblies.

The shaping or flattening of the flux in the cores was achieved by the use of reflector condition (i.e. light water) and by zoning (i.e. varying the fuel concentration or poison loading). Though the latter method is more effective but it also affects the neutron economy due to its high neutron absorption cross section.

The maximum to average flux ratio for both the cores is above 1 that is 2.807 for core 1 and 2.498 for core 2 indicating that the maximum heat generation rate is greater than those corresponding to average neutron flux. The maximum to average flux ratio determined for the UOX fueled core was greater than that to a standard AP1000 reactor (i.e. 2.3 value) determined based on the amount of the energy that can be safely carried by the coolant.

Reactor physics parameters: The delayed neutron fraction for the analysis was calculated by first determining the effective multiplication factor using the KCODE data card (refer Table 3.1) and then the prompt multiplication factor using the TOTNU card with a NO entry. The prompt multiplication factor ( $k_p$ ) for core 1 and core 2 were determined as  $1.11194 \pm 0.00015$  and  $1.11733 \pm 0.00017$  respectively.

Table 3.1. Reactor physics parameters for cores with LEU fuel arrangement.

Details	Core 1 : UOX-1/21-2.35/16-3.4/52-4.45	Core 2 : UOX-2/09-2.35/32-3.4/48-4.45
Effective Multiplication Factor	1.11945 ± 0.00014	1.12512 ± 0.00016
Maximum to Average Flux Ratio	2.807	2.498
Delayed Neutron Fraction	0.00671	0.0069
Control Rod Worth	0.1715	0.1570
Fuel Co-efficient of Reactivity ( $\delta k/^\circ\text{C}$ )	-2.58E-05	-2.42E-05
Moderator Co-efficient of Reactivity ( $\delta k/^\circ\text{C}$ )	-1.57E-03	-1.54E-03

Now using these values (i.e.  $k_{\text{eff}}$  and  $k_{\text{prompt}}$ ) in equation 2, the effective delayed neutron fraction ( $\beta_{\text{eff}}$ ) were calculated as 0.00671 for core 1 and 0.0069 for core 2. The  $\beta_{\text{eff}}$  values were found to be in good agreement with the standard value for six group delayed neutron fraction using the  $\text{U}^{235}$  fuel (Table 3.7). Furthermore the delayed neutron fraction can also be used to calculate the average neutron generation time (equation 3) in order to determine the rate at which power can rise during normal reactor operation.

The shutdown margin or the control rod worth is the amount of negative reactivity required by the reactor to become subcritical from its present condition. The control rod worth for normal shutdown condition (i.e. at 600K) were calculated as 0.1715 for core 1 and 0.1570 for core 2. Furthermore, the control rods were also checked for its ability to shut-down the reactor at cold operating conditions (i.e. at 300 K). At cold operating

conditions, the  $k_{\text{eff}}$  values for the cores with complete control rod insertions were calculated as 0.98178 for core 1 and 0.99996 for core 2 indicating a safe shut-down of the reactor and eliminating the need for any additional soluble boron poison.

From Table 3.1, the moderator reactivity co-efficient for core 1 and core 2 are  $-1.57\text{E-}03 \delta k/^{\circ}\text{C}$  and  $-1.54\text{E-}03 \delta k/^{\circ}\text{C}$ . The negative sign indicates the reactor is under moderated, as the moderator reactivity co-efficient is the function of fuel to moderator ratio. It is always desirable for the reactor to have a negative reactivity co-efficient due to its self-regulating effect. For any positive reactivity, this will increase the core temperatures thus resulting in introduction of large negative feedback reactivity thereby controlling the power and safely shutting down the reactor.

Now again from Table 3.1, the fuel reactivity co-efficient were calculated as  $-2.58\text{E-}05 \delta k/^{\circ}\text{C}$  for core 1 and  $-2.42\text{E-}05 \delta k/^{\circ}\text{C}$  for core2. The negative sign again indicates that for any positive reactivity the fuel temperature rises rapidly thus introducing a negative feedback reactivity and controlling the reactor to safety. A negative fuel reactivity co-efficient is more desirable than moderator reactivity co-efficient. This is because in case of a positive reactivity insertion, the time response for a negative feedback from moderator is comparatively slower than to the fuel. Hence the fuel reactivity co-efficient is also called as prompt reactivity co-efficient. Furthermore, the larger value of fuel reactivity co-efficient also leads to Doppler Effect or Doppler Broadening phenomenon for higher fuel temperatures.

Critical boron concentration: Figure 3.3 shows the boron ( $\text{B}^{10}$ ) concentration in ppm (parts per million) corresponding to the  $k_{\text{eff}}$  values for the UOX fueled cores. Based on the plot, the soluble boron concentration for reactor criticality (i.e.  $k_{\text{eff}} = 1$ ) was determined.

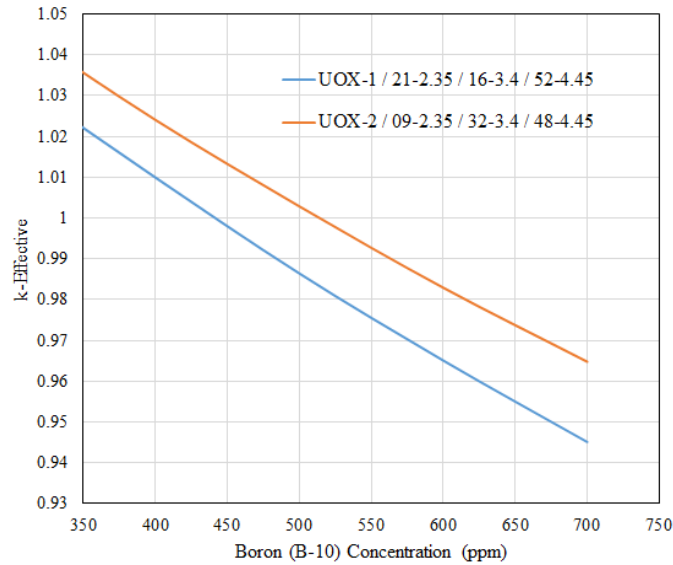


Figure 3.3. The k-effective vs boron ( $B^{10}$ ) concentration for UOX fueled cores.

For core 1 the critical boron (i.e.  $B^{10}$ ) concentration is 449.727 ppm whereas for core 2 the critical boron concentration is 508.339 ppm. Just like the control rods the soluble boron also plays a major role in controlling the reactor criticality during burn-up. In comparison to a standard  $UO_2$  PWR, the critical boron concentration for the UOX cores was higher which leads to a positive moderator temperature coefficient at higher coolant temperatures thus making the cores more prone to reactivity induced accidents. To overcome this effect it was necessary to introduce more burnable poison in the cores.

Another effect due to high critical boron concentration is the boron dilution accidents or any corrosion related damage to the reactor components due to long exposure to soluble boron.

Equilibrium cycle and spent nuclear fuel analysis: A three batch refueling strategy was adopted to determine the equilibrium cycle. Figures 3.4 and 3.5 shows the effective

multiplication factor ( $k_{eff}$ ) variation with burn time (days) for UOX fueled cores for once burn, twice burn and equilibrium cycle.

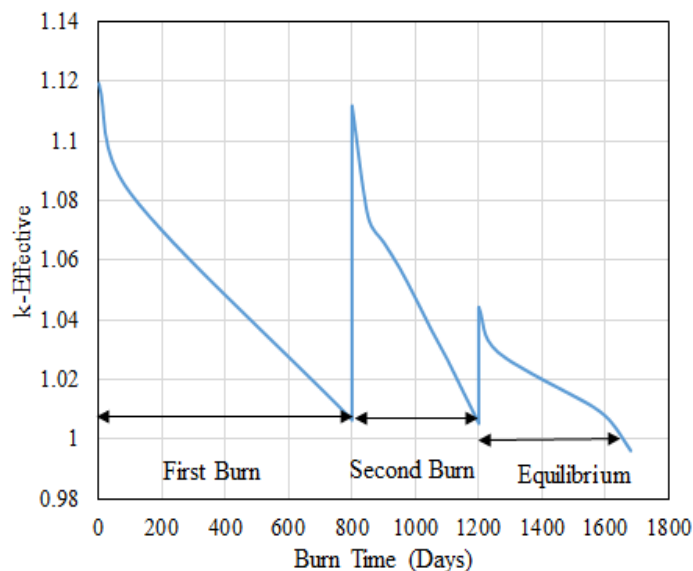


Figure 3.4. Three batch refueling cycle for UOX-1/21-2.35/16-3.4/52-4.45.

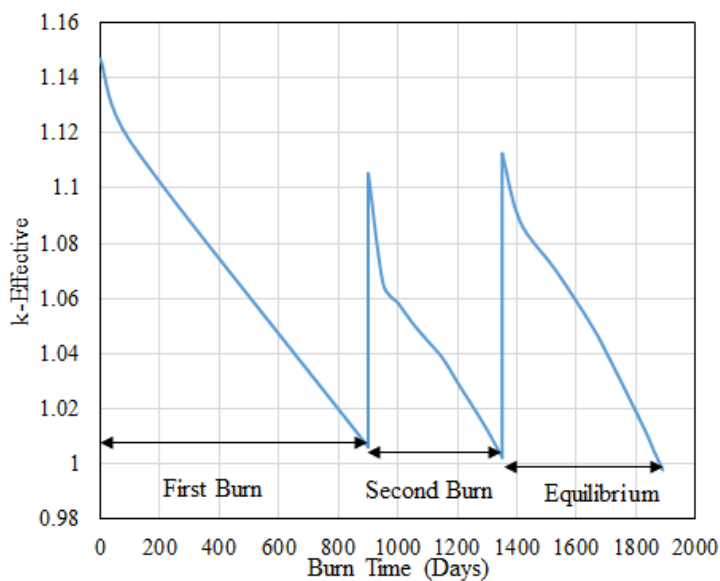


Figure 3.5. Three batch refueling cycle for UOX-2/09-2.35/32-3.4/48-4.45.

It is observed from the figures that the  $k_{\text{eff}}$  value in the both the cores drops sharply for the first 50 days of the burn cycle. This is due to xenon and samarium build-up after reactor start-up. Xenon is produced directly as fission product and also through beta decay of other fission product like  $\text{Te}^{135}$  (Tellurium) and  $\text{I}^{135}$  (Iodine), and has a half-life of about 9.2 hours. Its high neutron absorption cross section (i.e.  $\sigma_a = 2.65 \times 10^{-18} \text{ cm}^2$ ) results in large negative reactivity insertion in the reactor core. When the reactor core is fresh (i.e. at zero power), the amount of xenon concentration in the reactor is zero. But after the reactor start-up, the xenon concentration rapidly increases thus resulting in sharp decrease in  $k_{\text{eff}}$  value. After 50 days the xenon concentration eventually saturates and reaches equilibrium value. This in addition to the depletion of the other burnable poisons in the core results in monotonous decrease in the  $k_{\text{eff}}$  values. From the figures, the cycle length for the two UOX fueled cores are 800 days (~27 months) for once burn cycle, 400 days (~14 months) for twice burn cycle and 420 days (14 months) for equilibrium cycle for core 1 and 900 days (30 months) for once burn cycle, 450 days (15 months) for twice burn cycle and 510 days (17 months) for equilibrium cycle for core 2.

The spent fuel composition for the actinides at the end of equilibrium cycle are presented in the following Tables 3.2.

Table 3.2. Total actinide composition for the UOX fueled cores.

Fission Products	UOX-1/21-2.35/16-3.4/52- 4.45	UOX-2/09-2.35/32-3.4/48- 4.45
	Mass (kgs)	Mass (kgs)
$\text{U}^{235}$	459.7	355
$\text{U}^{236}$	100.7	119.3
$\text{U}^{238}$	26150	26080



Table 3.2. Total actinide composition for the UOX fueled cores (cont.)

Np <sup>237</sup>	7.972	10.41
Np <sup>239</sup>	2.041	2.018
Pu <sup>238</sup>	1.992	3.121
Pu <sup>239</sup>	164.8	163.9
Pu <sup>240</sup>	41.15	48.65
Pu <sup>241</sup>	22.49	26.46
Pu <sup>242</sup>	6.134	9.568
Am <sup>241</sup>	0.5743	0.8145
Am <sup>242</sup>	0.003307	0.004514
Am <sup>243</sup>	0.9838	1.647
Am <sup>244</sup>	0.000584	0.000845
Cm <sup>242</sup>	0.1389	0.2056
Cm <sup>243</sup>	0.002938	0.004108
Cm <sup>244</sup>	0.2452	0.4722
Cm <sup>245</sup>	0.01059	0.02135
Cm <sup>246</sup>	0.000785	0.002185

The Plutonium isotopes in the actinide composition are of principal interest due to its high potential for proliferation as well as high decay heat. But the composition for plutonium alone cannot be considered as a sole criteria for proliferation as the uranium and plutonium also co exists as a mixture in the composition. Though all the plutonium isotopes are radioactive but Pu<sup>239</sup> alone is responsible for proliferation but presence of high amount of Pu<sup>238</sup>, Pu<sup>240</sup> and Pu<sup>242</sup> in the spent fuel can counter this issue due to its high radioactivity and decay heat. The decay heat for each of the plutonium vectors in the spent fuel composition is presented in the following Table 3.3. The standard decay heat values are taken from reference 15. Table 3.4 shows the total non-actinide composition in the spent fuel for both the UOX fueled cores.

Table 3.3. Decay heat values for the Pu vectors in the UOX spent fuel.

Fission Products	Decay Heat (W/kg)	UOX-1/21-2.35/16-3.4/52-4.45		UOX-2/09-2.35/32-3.4/48-4.45	
		Mass (kgs)	Decay Heat (W)	Mass (kgs)	Decay Heat (W)
Pu <sup>238</sup>	560	1.992	1115.52	3.121	1747.76
Pu <sup>239</sup>	1.9	164.8	313.12	163.9	311.41
Pu <sup>240</sup>	6.8	41.15	279.82	48.65	330.82
Pu <sup>241</sup>	4.2	22.49	94.458	26.46	111.132
Pu <sup>242</sup>	0.1	6.134	0.6134	9.568	0.9568

Table 3.4. Total non-actinide composition for the UOX fueled cores.

Fission Products	UOX-1/21-2.35/16-3.4/52-4.45		UOX-2/09-2.35/32-3.4/48-4.45	
	Mass (kgs)		Mass (kgs)	
Mo <sup>95</sup>	11.54		14.8	
Tc <sup>99</sup>	16.43		18.99	
Ru <sup>101</sup>	15.93		18.27	
Rh <sup>105</sup>	8.92		9.778	
Ag <sup>109</sup>	1.143		1.208	
Cs <sup>133</sup>	24.13		29.03	
Nd <sup>143</sup>	17.14		19.24	
Nd <sup>145</sup>	14.49		16.83	
Sm <sup>147</sup>	1.514		1.966	
Sm <sup>149</sup>	0.06866		0.06167	
Sm <sup>150</sup>	5.454		6.441	
Sm <sup>151</sup>	0.2298		0.2178	
Sm <sup>152</sup>	2.251		2.619	
Gd <sup>155</sup>	1.317		1.534	
Gd <sup>155</sup>	0.00062		0.00075	
Total	120.55808		140.98622	

The total fission poisoning composition in UOX cores were 120.558 kgs for core 1 and 140.986 kgs for core 2. The fission product composition for each of these isotopes were used for burnup studies of non-actinides for cores with MOX and TRU fuels.

### 3.2. MIXED-OXIDE FUEL

Radial neutron flux profile: Figures 3.6 and 3.7 show the 2 dimensional radial neutron flux profile map for the MOX fueled cores. It can be observed that the thermal flux profile for the MOX cores is also uniformly distributed with the maximum flux observed at the central fuel assembly. On comparison with the UOX fueled cores, it was found that the flux values were higher basically due to higher fissile loading content in the MOX fueled cores. The uniform flux distribution as well as the flux flattening throughout the core was because of the intra-assembly zoning consisting of higher enrichment uranium and burnable absorbers along the core periphery.

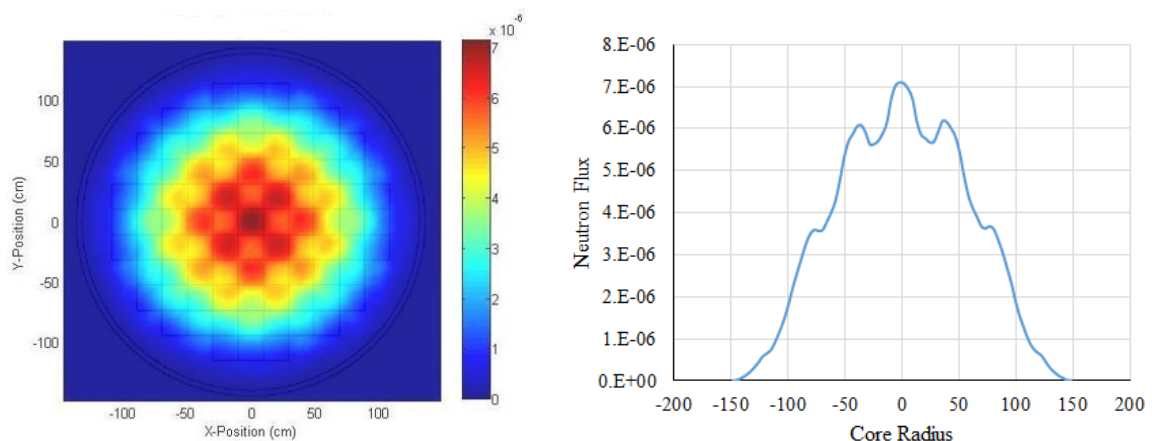


Figure 3.6. 2D-radial neutron flux profile for MOX-1/RG/25-4.5/40-4.2 /24- MOX.

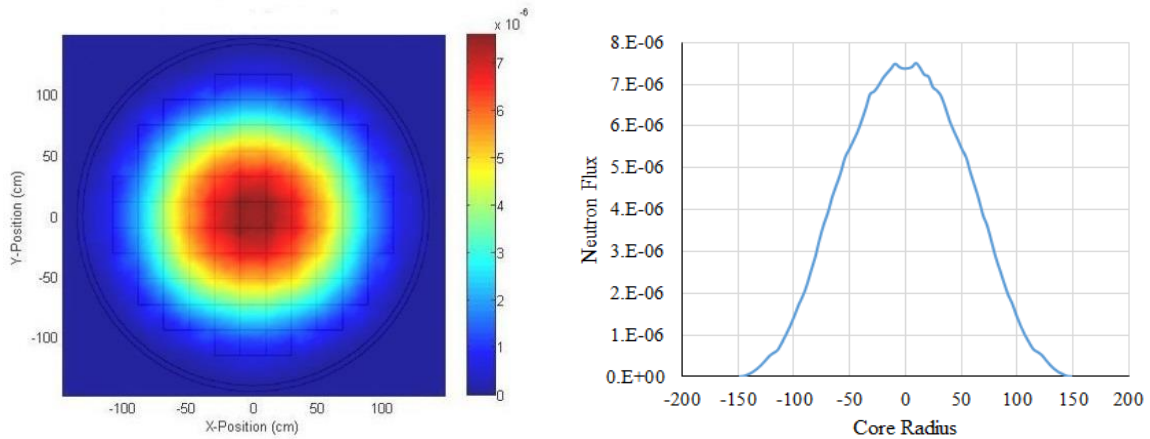


Figure 3.7. 2D-radial neutron flux profile for MOX-2/WG/25-4.5/40-4.2 /24- MOX.

The maximum to the average flux ratio for the MOX fueled cores were determined as 2.628 for core 1 and 2.752 for core 3 respectively.

Reactor physics parameters: Generally the delayed neutron fraction for MOX is always lower than the UOX fuel thus making the reactor control difficult during normal operating conditions and transient conditions. From Table 3.5, the delayed neutron fraction for core 1 and core 3 were calculated as 2.628 and 2.752 respectively which were found to be in good agreement with the standard value of six group delayed neutron fraction for Pu<sup>239</sup> isotope.

The control worth calculated for core 1 and 2 are 0.26347 and 0.199626 as shown in Table 3.5. It is observed the control rod worth or the shutdown margin for the MOX fuel is comparatively greater than that of UOX fuel. This is because the plutonium in the MOX fuel exhibits a higher thermal neutron absorption cross section compared to that of uranium. This hardening of neutron spectrum decreases the neutron absorption by control rods or burnable poison thus reducing the control rod or absorber worth.

The reactivity co-efficient values for fuel and moderator for core 1 (i.e.  $-2.86E-05 \delta k/^{\circ}C$  and  $-1.46E-03 \delta k/^{\circ}C$ ) and for core 2 (i.e.  $-2.64E-05 \delta k/^{\circ}C$  and  $-1.37E-03 \delta k/^{\circ}C$ ) are shown in Table 3.5. The negative sign again indicates that for a positive reactivity, the power and temperature rises thus leading to large negative feedback reactivity introduction and controlling the reactor to safety. Compared to the UOX fuel, the reactivity co-efficient for MOX cores are less negative. This is because of lower capture resonance and high absorption resonance for  $Pu^{239}$ . This increase in neutron absorption means increased fission thus resulting in positive reactivity and making the reactivity co efficient less negative.

Table 3.5. Reactor physics parameters for cores with MOX fuel arrangement.

Details	Core 1 : MOX-1 /RG/25-4.5/40-4.2 /24- MOX	Core 2 : MOX-2 /WG/25-4.5/40-4.2 /24- MOX
Multiplication Factor	$1.14509 \pm 0.00016$	$1.11126 \pm 0.00015$
Maximum to Average Flux Ratio	2.628	2.752
Delayed Neutron Fraction	0.005834	0.004778
Control Rod Worth (Integral Method)	0.26347	0.199626
Fuel Co-efficient of Reactivity ( $\delta k/^{\circ}C$ )	$-2.86E-05$	$-2.64E-05$
Moderator Co-efficient of Reactivity ( $\delta k/^{\circ}C$ )	$-1.46E-03$	$-1.37E-03$

Critical boron concentration: Figure 3.8 shows the soluble boron ( $B^{10}$ ) concentration in ppm corresponding to the  $k_{\text{eff}}$  values for MOX fueled cores.

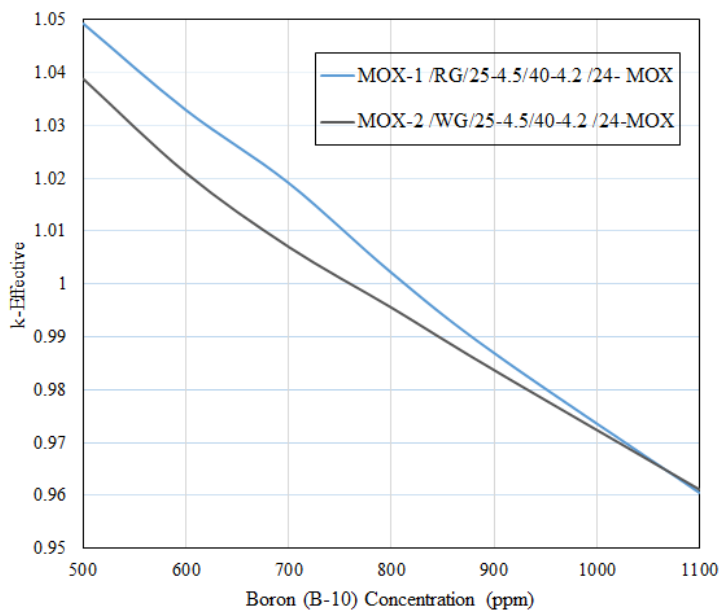


Figure 3.8. The k-effective vs boron ( $B^{10}$ ) concentration for MOX fueled cores.

The critical boron concentration for reactor criticality for core 1 and core 2 are 813.958 ppm and 752.334 ppm. It is observed that the critical boron concentration for MOX cores is much greater than that to the UOX cores. This is due to the high initial  $Pu^{240}$  content in the fuel assembly which leads to the formation of  $Pu^{241}$  isotope thus introducing more positive reactivity in the core, and also to overcome the lower negative moderator coefficient.

Equilibrium cycle and spent nuclear fuel analysis: Figures 3.9 and 3.10 shows the variation in effective multiplication factor for MOX fueled cores (i.e. reactor and weapon grade) for once burn, twice burn and equilibrium cycle.

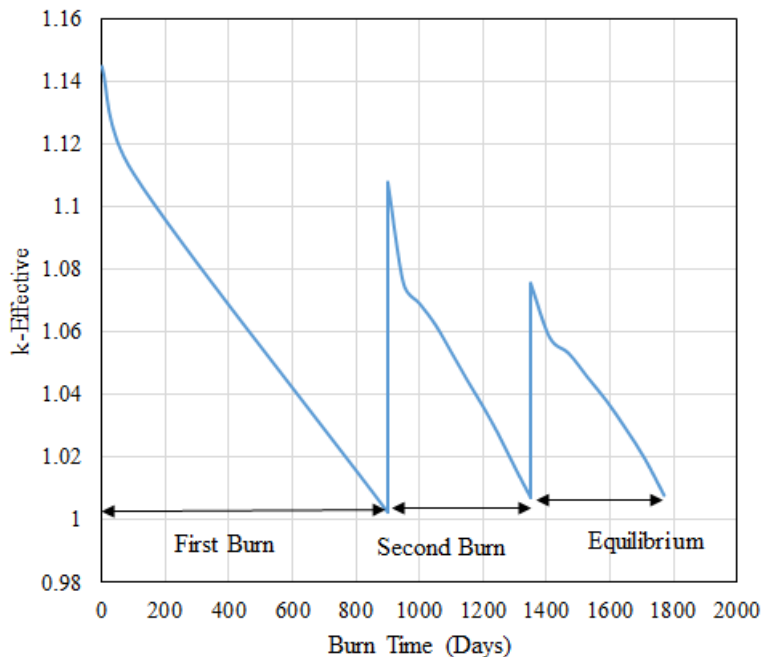


Figure 3.9. Three batch refueling cycle for MOX-1/RG/25-4.5/40-4.2/24- MOX.

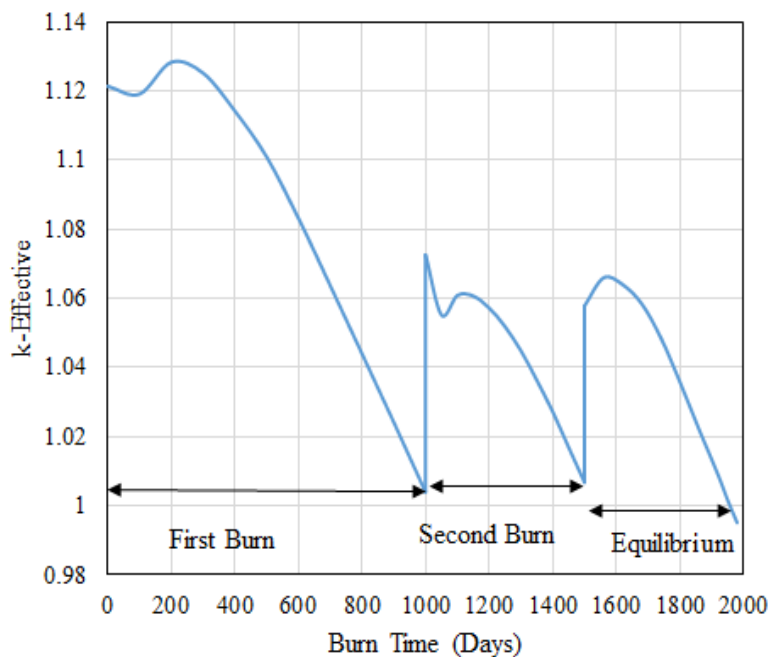


Figure 3.10. Three batch refueling cycle for MOX-3/WG/25-4.5/40-4.2/24- MOX.

From the Figure 3.9 it is observed the burn characteristics for the MOX core with reactor grade plutonium is similar to that with the UOX cores. That is the effective multiplication factor first drops sharply due to fission poison (i.e. xenon and samarium) build-up after reactor start-up, and then monotonously decreases once the amount of xenon and samarium concentration reaches the equilibrium value. On the other hand, the MOX core with weapons grade plutonium exhibits a different behavior where after the initial drop the multiplication factor increase before linearly decreasing again. This increase in  $k_{\text{eff}}$  value is due to higher fissile content in the form of  $U^{235}$ ,  $Pu^{239}$  and  $Pu^{241}$  and also due to high  $Pu^{240}$  content which on burnup gets converted to  $Pu^{241}$  thus adding up to more positive reactivity in the core for the first 200 days of the burn cycle. From the figures, the cycle length for the two MOX fueled cores are 900 days (30 months) for once burn cycle, 450 days (15 months) for twice burn cycle and 420 days (14 months) for equilibrium cycle for core 1 and 1000 days (~33 months) for once burn cycle, 500 days (~16 months) for twice burn cycle and 450 days (15 months) for equilibrium cycle for core2.

The burn-up characteristics for the MOX fuel is smaller compared to that for UOX fuel. It is observed that the total actinide composition is decreased due to high initial composition of  $Pu^{240}$  in the MOX assembly and better conversion factor. The high  $Pu^{240}$  content in the reactor core exhibits high rate of spontaneous fission resulting in high neutron emission and heat generation thus making the spent fuel highly undesirable for proliferation. Tables 3.6 and 3.7 presents the fuel utilization at the end of equilibrium cycle in the MOX fuel assembly with reactor grade and weapon grade plutonium.



Table 3.6. Initial and final actinide composition for the reactor grade MOX fuel assembly.

Fission Products	Initial Composition	Final Composition
	Mass (kgs)	Mass (kgs)
U <sup>235</sup>	4.762	0.752
Pu <sup>238</sup>	1.971	1.647
Pu <sup>239</sup>	58.162	24.351
Pu <sup>240</sup>	23.653	17.167
Pu <sup>241</sup>	10.758	10.142
Pu <sup>242</sup>	4.928	10.897

Table 3.7. Initial and final actinide composition for the weapon grade MOX fuel assembly.

Fission Products	Initial Composition	Final Composition
	Mass (kgs)	Mass (kgs)
U <sup>235</sup>	4.762	0.674
Pu <sup>238</sup>	0	0.853
Pu <sup>239</sup>	92.348	24.566
Pu <sup>240</sup>	5.821	16.475
Pu <sup>241</sup>	1.166	9.567
Pu <sup>242</sup>	0.099	6.596

It is also observed that the overall Pu<sup>239</sup> content utilization at the end of equilibrium cycle in the reactor grade MOX assembly is approximately 58 percent whereas in the

weapon grade MOX assembly is approximately 74 percent. Though the Am<sup>241</sup> poisoned is enhanced (i.e. 2.861 kgs for core 1 and 2.102 kgs for core 3) in the MOX assembly again owing to high initial Pu<sup>240</sup> content, but it is well below the limiting value which is less than 3 percent of the total actinide composition (i.e. due to its high radioactivity) thus making it possible to separate the reactor grade plutonium from the spent fuel and reuse it to fabricate MOX fuel assemblies.

Table 3.8 shows the composition of the most stable, non-volatile and neutron absorbing fission products for the MOX fuel. These fission products constitute 78 percent of the total poisoning in the MOX fuel and exhibits similar burn characteristics to that in UOX fuel except for few modifications.

Table 3.8. Total non-actinide composition for the MOX fueled cores.

Fission Products	MOX-1 /RG/25-4.5/40-4.2	MOX-2 /WG/25-4.5/40-4.2
	/24- MOX	/24- MOX
	Mass (kgs)	Mass (kgs)
Mo <sup>95</sup>	12.15	14.36
Tc <sup>99</sup>	17.05	20.36
Ru <sup>101</sup>	17.06	20.81
Rh <sup>105</sup>	10.28	12.91
Ag <sup>109</sup>	1.755	2.303
Cs <sup>133</sup>	27.08	29.82
Nd <sup>143</sup>	17.71	20.48
Nd <sup>145</sup>	14.7	17.1
Sm <sup>147</sup>	1.55	1.835
Sm <sup>149</sup>	0.08158	0.0821
Sm <sup>150</sup>	6.154	7.204
Sm <sup>151</sup>	0.2807	0.2956

Table 3.8. Total non-actinide composition for the MOX fueled cores (cont.)

Sm <sup>152</sup>	2.452	2.77
Gd <sup>155</sup>	1.764	1.884
Gd <sup>155</sup>	0.001242	0.0014
Total	130.0685	152.2151

First it was observed, the fission product worth was reduced particularly for Nd<sup>143</sup>, Gd<sup>155</sup>, Sm<sup>149</sup> and Sm<sup>151</sup> isotopes. This was due to hardened neutron spectrum induced by plutonium isotopes which reduces the neutron capture ability of fission products in the thermal energy range thus reducing the absorber worth. Another important difference observed was the cumulative fission product yield due to U<sup>235</sup> fission and Pu<sup>239</sup>/Pu<sup>241</sup> fission. The yields of Mo<sup>95</sup>, Nd<sup>143</sup> and Nd<sup>145</sup> are reduced with Pu<sup>239</sup>/Pu<sup>241</sup> fission thus reducing the negative worth of these fission poisons. On the other hand the negative worth for Rh<sup>103</sup>, Ag<sup>109</sup> and Eu<sup>153</sup> were enhanced in the MOX pellet due to its increased fission yield with the plutonium isotopes

### 3.3. TRANSURANIC FUEL

Radial neutron flux profile: Figure 3.11 shows the 2 dimensional radial neutron flux profile for TRU fueled core. The flux profile is similar to that of UOX and MOX cores.

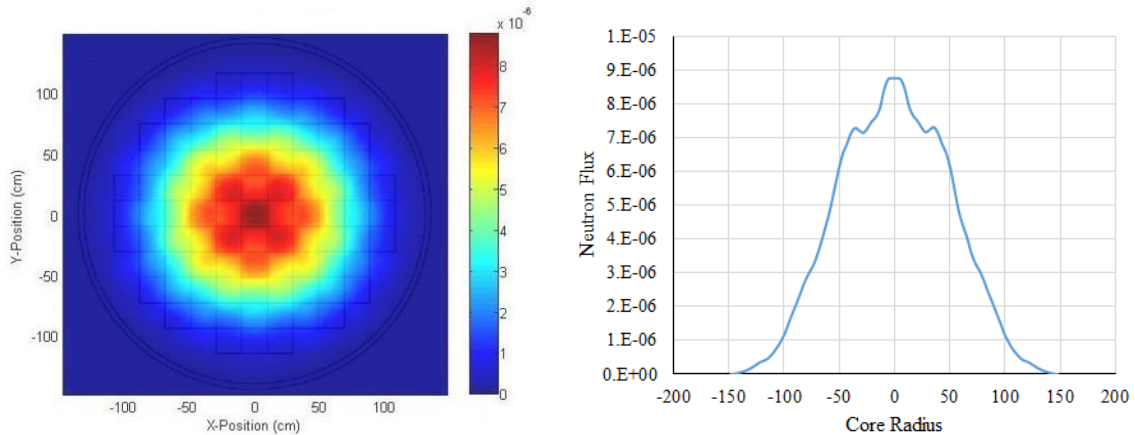


Figure 3.11. 2D-radial neutron flux profile for TRU-1/25-4.5/40-4.2/24- TRU.

The flux is again uniformly distributed throughout the core with the maximum flux at the central fuel assembly. The maximum to average flux ratio was calculated as 2.535.

Reactor physics parameter: The delayed neutron fraction for TRU fuel was calculated as 0.004822 as shown in Table 3.9 which is similar to MOX fuel due to the presence of  $\text{Pu}^{239}$  in the TRU fuel assemblies.

The control worth calculated for TRU core is calculated as 0.23961. It is observed the control rod worth or the shutdown margin for the TRU fuel is similar to that of MOX fuel. This is because the higher plutonium content in the TRU fuel which also exhibits a higher thermal neutron absorption cross section thus resulting in the decrease of neutron absorption by control rods or burnable poison.

The reactivity co-efficient values for fuel and moderator for TRU core are  $-1.43\text{E-}05 \delta k/^\circ\text{C}$  and  $-1.135\text{E-}03 \delta k/^\circ\text{C}$  as shown in Table 3.8. Compared to UOX fuel the reactivity co-efficient for TRU cores are also less negative. This is again because of low capture resonance and high absorption resonance for  $\text{Pu}^{239}$  which results in positive reactivity thus making the reactivity co-efficient less negative.

Table 3.9. Reactor physics parameters for cores with TRU fuel arrangement.

Details	Core 1 : TRU-1 /25-4.5/40-4.2 /24-TRU
Multiplication Factor	$1.21939 \pm 0.00012$
Maximum to Average Flux Ratio	2.535
Delayed Neutron Fraction	0.004822
Control Rod Worth	0.23961
Fuel Co-efficient of Reactivity ( $\delta k/^\circ\text{C}$ )	-1.430E-05
Moderator Co-efficient of Reactivity ( $\delta k/^\circ\text{C}$ )	-1.135E-03

Critical boron concentration: Figure 3.12 shows the soluble boron ( $\text{B}^{10}$ ) concentration in ppm corresponding to the  $k_{\text{eff}}$  values for TRU fueled cores. The critical boron concentration for reactor criticality for TRU core is 1547.807 ppm. It is observed that the critical boron concentration for TRU core is greater than that to the UOX and MOX cores to overcome the presence and formation of plutonium isotopes and the long lived fission products (i.e. trans-uranic actinides) in the fuel assembly.

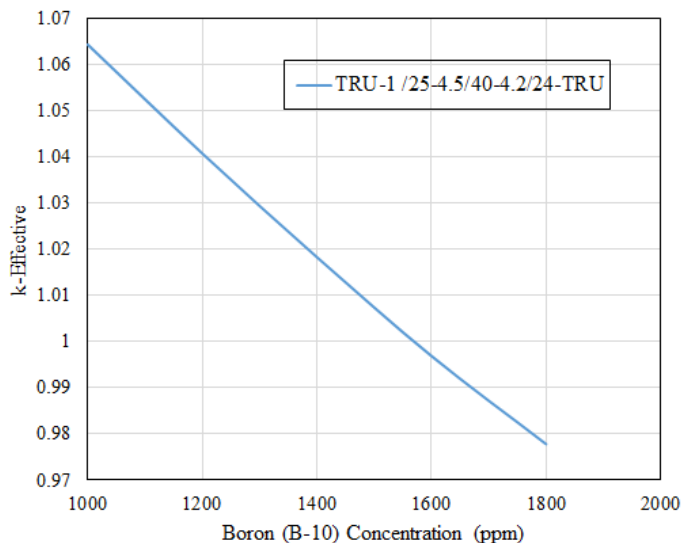


Figure 3.12. The k-effective vs boron ( $B^{10}$ ) concentration for TRU fueled core.

Equilibrium cycle and spent nuclear fuel analysis: Figure 3.13 shows the multiplication factor variation for TRU fueled core for once, twice and equilibrium burn cycle.

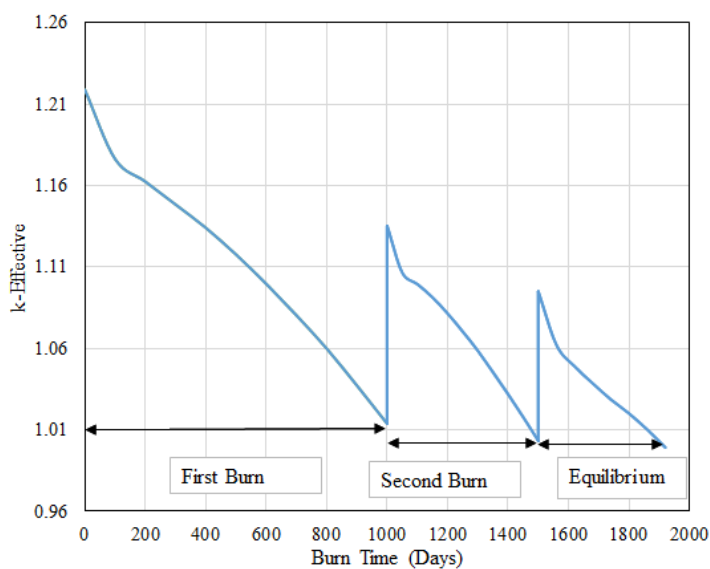


Figure 3.13. Three batch refueling cycle for TRU-1/25-4.5/40-4.2/24-TRU.

The burn characteristic for the TRU fueled core stands in good agreement with the UOX fueled cores. From the figure, the cycle length for the TRU core is 1000 days (~33 months) for once burn cycle, 500 days (~16 months) for twice burn cycle and 360 days (12 months) for equilibrium cycle.

Table 3.10 shows the fuel utilization at the end of equilibrium cycle in the TRU fuel assembly, whereas Table 3.11 shows the non-actinide composition in the spent fuel for the TRU fueled core. The burnup analysis for the TRU fuel is also different compared to UOX and MOX cores in terms of its actinide composition.

Table 3.10. Initial and final actinide composition for the TRU fuel assembly.

Fission Products	Initial Composition	Final Composition
	Mass (kgs)	Mass (kgs)
Np <sup>237</sup>	10.36	2.25
Pu <sup>238</sup>	2.941	7.842
Pu <sup>239</sup>	135	4.303
Pu <sup>240</sup>	42.3	13.39
Pu <sup>241</sup>	14.34	9.254
Pu <sup>242</sup>	7.703	17.53
Am <sup>241</sup>	9.916	1.079
Am <sup>242</sup>	0.00669	0.00667
Am <sup>243</sup>	1.297	5.291
Cm <sup>242</sup>	0.00002	0.6154
Cm <sup>243</sup>	0.00283	0.04654
Cm <sup>244</sup>	0.188	5.671
Cm <sup>245</sup>	0.1134	0.4734
Cm <sup>246</sup>	0.0009	0.2623

Just like the MOX assembly, the high initial Pu<sup>240</sup> content decreases the actinide composition in the TRU fuel and also enhances the Am<sup>241</sup> poisoning. It is observed from the table that the total Am<sup>241</sup> consumption at the end of equilibrium cycle is more than 89 percent. This is important in criticality analysis for storage and disposal of spent fuel due to high radioactivity effects of Am<sup>241</sup> and Np<sup>237</sup> formed due to its  $\alpha$ -decay which induces a large negative reactivity in the spent fuel. The overall Pu<sup>239</sup> consumption of more than 94 percent. The total consumption for the Am and Np consumption was 43 percent and 78 percent respectively. These values were in good agreement with the reference values based on the burnup characteristics for inert matrix TRU fuels.

Table 3.11. Total non-actinide composition for the TRU fueled core.

Fission Products	TRU-1 /25-4.5/40-4.2 /24- TRU
	Mass (kgs)
Mo <sup>95</sup>	13.07
Tc <sup>99</sup>	18.34
Ru <sup>101</sup>	19.17
Rh <sup>105</sup>	11.93
Ag <sup>109</sup>	2.379
Cs <sup>133</sup>	26.51
Nd <sup>143</sup>	18.54
Nd <sup>145</sup>	15.49
Sm <sup>147</sup>	1.51
Sm <sup>149</sup>	0.08416
Sm <sup>150</sup>	6.353
Sm <sup>151</sup>	0.3163
Sm <sup>152</sup>	2.59
Gd <sup>155</sup>	1.904
Gd <sup>155</sup>	0.001301
Total	138.1878



The burnup characteristics for the fission products (i.e. non-actinides) in the TRU cores is similar to that for MOX cores. This is because of high initial plutonium content particularly for  $\text{Pu}^{239}$ ,  $\text{Pu}^{240}$  and  $\text{Pu}^{241}$  isotopes in the TRU fuel assemblies. The total composition of the fission products as well for important individual isotopes were in good agreement with that for MOX assemblies.

#### 4. CONCLUSION

The Westinghouse SMR was modelled and analyzed with flexible fuel configurations using the Monte Carlo N-Particle code. The fuels investigated in the study were uranium-oxide, mixed-oxide and trans-uranic fuels. First, the SMR core was referenced with the UOX fuel assembly; and on confirming good performance it was then used for the comparative study with other fuel options. The study was carried out by determining the reactor physics parameters (i.e. the radial flux profile and the delayed neutron fraction) and the reactor safety related parameters (i.e. the temperature co-efficient, the soluble boron and control rod worth) at BOL. Furthermore, the spent fuel composition for each of these oxide fueled cores was also analyzed.

For the UOX fueled cores, the parameters were in good agreement with that to the values for a standard pressurized water reactor with  $UO_2$  fuel. The radial neutron flux profile was uniformly distributed throughout the core. The control rod worth were sufficient to safely shutdown the reactor during normal as well as cold operating conditions. Furthermore, the soluble boron concentration was found to be within permissible limits thus controlling the criticality during reactor operation without resulting in corrosive damage to the reactor components. The reactivity co-efficient values for the fuel and moderator were also largely negative indicating a large negative feedback for any positive reactivity insertion thus controlling and safely shutting down the reactor.

Upon successful referencing the UOX fueled SMR, the core was analyzed with MOX and TRU fuels using the same procedure. Comparatively, the reactor physics parameter as well as the reactor safety parameters were found to be in good agreement with that to the UOX core. The delayed neutron fraction for the MOX and TRU fuel was lower

due to high initial plutonium content. Furthermore, the control rod and absorber worth was increased whereas the reactivity co-efficient were less negative. This was because of neutron spectrum hardening behavior exhibited by plutonium isotopes which decreased the neutron absorption by control rods and soluble boron thereby leading to positive reactivity insertion and reducing their worth.

The equilibrium cycle for each cores were also determined using a three batch refueling strategy. For the UOX cores, the equilibrium cycle length was 14 to 17 months whereas for MOX and TRU cores were 14 to 15 months and 12 months respectively. The 24 month refueling defined in the objective can be achieved by adopting a different core arrangement or by adjusting the boron concentration in the burnable absorbers or by increasing the fissile loading in the core. In the spent fuel, the composition for fissile material, the long lived and short lived isotopes were determined. This is highly recommended for the criticality analysis required for the storage of spent fuel which as a part of the future works to be conducted. In the MOX fueled cores, the reactor grade Pu consumption was 54 percent whereas weapon grade Pu consumption was 74 percent. The presence of high Pu<sup>20</sup> content enhanced the Am<sup>241</sup> poisoning but below the 3 percent safety criteria thus making it possible to separate and the recycle the spent fuel for MOX fuel fabrication. In TRU fuel, with the IMF based fuel Pu<sup>239</sup> consumption of 94 percent was achieved whereas the total Am and Np consumption were 43 percent and 78 percent respectively.

#### 4.1. FUTURE WORKS

For the future works, the first objective will be to completely analyze the spent

fuel composition for each of these cores for its radioactivity and decay heat using the ORIGEN code. These are important parameters required for criticality analysis of spent fuel for its storage and disposal. Furthermore, the cores also needs to be analyzed for its thermal-hydraulic behavior pertaining to reactor safety during normal operating conditions as well as transient conditions. Once the cores are analyzed, it is also necessary to validate the results using a different simulation code. Due to time constraint only three oxide fuels were analyzed but there is also a need to analyze the SMR core with other advanced fuel options like the non-oxide fuels using a similar approach.

## APPENDIX A

Spent fuel composition for LEU fuels after shutdown cooling for 10 years.

<b>ZAID</b>	<b>Mass (gm)</b>	<b>Activity (Ci)</b>	<b>Sp. Act. (Ci/gm)</b>	<b>Atom Den. (a/b-cm)</b>	<b>Atom Fr.</b>	<b>Mass Fr.</b>
<b>Actinide Inventory</b>						
90232	3.94E-03	4.32E-10	1.10E-07	3.77E-11	5.34E-10	1.40E-09
92233	5.67E-03	5.46E-05	9.64E-03	5.39E-11	7.65E-10	2.02E-09
92234	3.57E+01	2.22E-01	6.22E-03	3.39E-07	4.80E-06	1.27E-05
92235	2.93E+04	6.33E-02	2.16E-06	2.77E-04	3.92E-03	1.04E-02
92236	1.38E+04	8.89E-01	6.47E-05	1.29E-04	1.83E-03	4.89E-03
92238	2.33E+06	7.84E-01	3.36E-07	2.17E-02	3.08E-01	8.29E-01
93236	4.17E-03	5.49E-05	1.32E-02	3.92E-11	5.55E-10	1.48E-09
93237	1.20E+03	8.47E-01	7.05E-04	1.12E-05	1.59E-04	4.27E-04
94238	3.42E+02	5.86E+03	1.71E+01	3.19E-06	4.52E-05	1.22E-04
94239	1.57E+04	9.71E+02	6.20E-02	1.45E-04	2.06E-03	5.57E-03
94240	4.89E+03	1.11E+03	2.27E-01	4.52E-05	6.41E-04	1.74E-03
94241	1.66E+03	1.72E+05	1.03E+02	1.53E-05	2.17E-04	5.91E-04
94242	8.94E+02	3.54E+00	3.95E-03	8.19E-06	1.16E-04	3.18E-04
94244	1.36E-02	2.48E-07	1.83E-05	1.23E-10	1.75E-09	4.82E-09
95241	1.15E+03	3.94E+03	3.43E+00	1.06E-05	1.50E-04	4.09E-04
95242	7.77E-01	8.14E+00	1.05E+01	7.12E-09	1.01E-07	2.76E-07
95243	1.50E+02	3.00E+01	2.00E-01	1.37E-06	1.95E-05	5.35E-05
96242	2.04E-03	6.74E+00	3.31E+03	1.87E-11	2.64E-10	7.24E-10
96243	3.26E-01	1.69E+01	5.16E+01	2.98E-09	4.22E-08	1.16E-07
96244	2.18E+01	1.76E+03	8.09E+01	1.98E-07	2.81E-06	7.75E-06
96245	1.32E+00	2.26E-01	1.72E-01	1.19E-08	1.69E-07	4.68E-07
96246	1.04E-01	3.19E-02	3.07E-01	9.35E-10	1.33E-08	3.69E-08
<b>Non Actinide Inventory</b>						
6012	8.89E-01	0.00E+00	0.00E+00	1.64E-07	2.33E-06	3.16E-07
6013	1.98E+01	0.00E+00	0.00E+00	3.39E-06	4.80E-05	7.06E-06
7015	4.94E-02	0.00E+00	0.00E+00	7.30E-09	1.04E-07	1.76E-08
8016	3.37E+05	0.00E+00	0.00E+00	4.68E-02	6.63E-01	1.20E-01
8017	1.30E-01	0.00E+00	0.00E+00	1.69E-08	2.40E-07	4.61E-08
31069	3.42E-04	0.00E+00	0.00E+00	1.10E-11	1.56E-10	1.22E-10
31071	2.81E-03	0.00E+00	0.00E+00	8.78E-11	1.25E-09	9.99E-10
32072	7.70E-03	0.00E+00	0.00E+00	2.37E-10	3.37E-09	2.74E-09

32073	1.93E-02	0.00E+00	0.00E+00	5.88E-10	8.33E-09	6.87E-09
32074	5.57E-02	0.00E+00	0.00E+00	1.67E-09	2.37E-08	1.98E-08
32076	3.81E-01	0.00E+00	0.00E+00	1.11E-08	1.58E-07	1.35E-07
33075	3.09E-01	0.00E+00	0.00E+00	9.14E-09	1.30E-07	1.10E-07
34076	6.96E-03	0.00E+00	0.00E+00	2.03E-10	2.88E-09	2.47E-09
34077	9.62E-01	0.00E+00	0.00E+00	2.77E-08	3.93E-07	3.42E-07
34078	2.80E+00	0.00E+00	0.00E+00	7.97E-08	1.13E-06	9.96E-07
34079	5.77E+00	7.92E-01	1.37E-01	1.62E-07	2.30E-06	2.05E-06
34080	1.54E+01	0.00E+00	0.00E+00	4.28E-07	6.06E-06	5.48E-06
34082	4.14E+01	1.30E-15	3.13E-17	1.12E-06	1.59E-05	1.47E-05
35079	1.20E-03	0.00E+00	0.00E+00	3.36E-11	4.76E-10	4.25E-10
35081	5.77E+01	0.00E+00	0.00E+00	1.58E-06	2.24E-05	2.05E-05
36082	1.49E+00	0.00E+00	0.00E+00	4.04E-08	5.72E-07	5.30E-07
36083	1.24E+02	0.00E+00	0.00E+00	3.32E-06	4.70E-05	4.41E-05
36084	3.32E+02	0.00E+00	0.00E+00	8.76E-06	1.24E-04	1.18E-04
36085	1.58E+01	6.22E+03	3.93E+02	4.14E-07	5.86E-06	5.63E-06
36086	5.94E+02	0.00E+00	0.00E+00	1.53E-05	2.17E-04	2.11E-04
37085	2.86E+02	0.00E+00	0.00E+00	7.46E-06	1.06E-04	1.02E-04
37087	7.69E+02	6.59E-05	8.57E-08	1.96E-05	2.78E-04	2.74E-04
38086	8.83E-01	0.00E+00	0.00E+00	2.28E-08	3.23E-07	3.14E-07
38087	3.47E-03	0.00E+00	0.00E+00	8.85E-11	1.26E-09	1.23E-09
38088	4.25E+02	0.00E+00	0.00E+00	1.07E-05	1.52E-04	1.51E-04
39089	1.26E+03	0.00E+00	0.00E+00	3.14E-05	4.44E-04	4.47E-04
40090	4.39E+01	0.00E+00	0.00E+00	1.08E-06	1.54E-05	1.56E-05
40091	1.67E+03	0.00E+00	0.00E+00	4.07E-05	5.77E-04	5.93E-04
40092	1.92E+03	0.00E+00	0.00E+00	4.63E-05	6.56E-04	6.82E-04
40093	2.08E+03	5.23E+00	2.52E-03	4.97E-05	7.04E-04	7.40E-04
40094	2.29E+03	0.00E+00	0.00E+00	5.40E-05	7.65E-04	8.13E-04
40096	2.23E+03	0.00E+00	0.00E+00	5.16E-05	7.31E-04	7.93E-04
41093	1.72E-03	0.00E+00	0.00E+00	4.10E-11	5.81E-10	6.10E-10
41094	2.22E-03	4.17E-04	1.88E-01	5.25E-11	7.44E-10	7.90E-10
42094	1.62E-02	0.00E+00	0.00E+00	3.82E-10	5.41E-09	5.74E-09
42095	1.91E+03	0.00E+00	0.00E+00	4.46E-05	6.33E-04	6.79E-04
42096	6.93E+01	0.00E+00	0.00E+00	1.60E-06	2.27E-05	2.46E-05
42097	9.76E+02	0.00E+00	0.00E+00	2.23E-05	3.17E-04	3.47E-04
42098	9.90E+02	0.00E+00	0.00E+00	2.24E-05	3.18E-04	3.52E-04
42100	1.14E+03	0.00E+00	0.00E+00	2.53E-05	3.59E-04	4.06E-04
43099	2.10E+03	3.59E+01	1.71E-02	4.70E-05	6.66E-04	7.45E-04
44099	1.15E-01	0.00E+00	0.00E+00	2.58E-09	3.65E-08	4.08E-08
44100	1.55E+02	0.00E+00	0.00E+00	3.44E-06	4.87E-05	5.50E-05

44101	2.00E+03	0.00E+00	0.00E+00	4.40E-05	6.23E-04	7.11E-04
44102	9.75E+02	0.00E+00	0.00E+00	2.12E-05	3.01E-04	3.47E-04
44104	7.37E+02	0.00E+00	0.00E+00	1.57E-05	2.23E-04	2.62E-04
45103	1.11E+03	0.00E+00	0.00E+00	2.39E-05	3.39E-04	3.95E-04
46104	3.16E+02	0.00E+00	0.00E+00	6.75E-06	9.57E-05	1.12E-04
46105	7.88E+02	0.00E+00	0.00E+00	1.67E-05	2.36E-04	2.80E-04
46106	2.53E+02	0.00E+00	0.00E+00	5.29E-06	7.50E-05	8.98E-05
46107	2.74E+02	1.41E-01	5.15E-04	5.69E-06	8.06E-05	9.75E-05
46108	2.04E+02	0.00E+00	0.00E+00	4.19E-06	5.93E-05	7.24E-05
46110	6.85E+01	0.00E+00	0.00E+00	1.38E-06	1.96E-05	2.44E-05
47109	1.12E+02	0.00E+00	0.00E+00	2.27E-06	3.22E-05	3.97E-05
48110	2.83E+01	0.00E+00	0.00E+00	5.71E-07	8.09E-06	1.01E-05
48111	3.20E+01	0.00E+00	0.00E+00	6.39E-07	9.06E-06	1.14E-05
48112	1.70E+01	0.00E+00	0.00E+00	3.38E-07	4.78E-06	6.05E-06
48113	3.08E-01	1.05E-13	3.41E-13	6.05E-09	8.58E-08	1.10E-07
48114	1.48E+01	0.00E+00	0.00E+00	2.87E-07	4.08E-06	5.25E-06
48116	5.55E+00	0.00E+00	0.00E+00	1.06E-07	1.51E-06	1.97E-06
49115	2.41E+00	1.70E-11	7.06E-12	4.66E-08	6.60E-07	8.58E-07
50115	2.30E-01	0.00E+00	0.00E+00	4.45E-09	6.30E-08	8.19E-08
50116	1.54E+00	0.00E+00	0.00E+00	2.96E-08	4.19E-07	5.49E-07
50117	5.01E+00	0.00E+00	0.00E+00	9.52E-08	1.35E-06	1.78E-06
50118	2.22E+00	0.00E+00	0.00E+00	4.17E-08	5.91E-07	7.87E-07
50119	4.66E+00	0.00E+00	0.00E+00	8.69E-08	1.23E-06	1.66E-06
50120	8.01E+00	0.00E+00	0.00E+00	1.48E-07	2.10E-06	2.85E-06
50122	5.78E+00	0.00E+00	0.00E+00	1.05E-07	1.49E-06	2.06E-06
50124	5.14E+00	0.00E+00	0.00E+00	9.19E-08	1.30E-06	1.83E-06
51121	4.42E+00	0.00E+00	0.00E+00	8.11E-08	1.15E-06	1.57E-06
51123	5.75E+00	0.00E+00	0.00E+00	1.04E-07	1.47E-06	2.05E-06
52122	1.28E-01	0.00E+00	0.00E+00	2.32E-09	3.29E-08	4.54E-08
52123	7.33E-04	1.72E-13	2.35E-10	1.32E-11	1.87E-10	2.60E-10
52124	7.55E-02	0.00E+00	0.00E+00	1.35E-09	1.92E-08	2.69E-08
52125	1.74E+00	0.00E+00	0.00E+00	3.10E-08	4.39E-07	6.20E-07
52126	6.14E-01	0.00E+00	0.00E+00	1.08E-08	1.53E-07	2.18E-07
52128	1.10E+02	0.00E+00	0.00E+00	1.91E-06	2.71E-05	3.92E-05
52130	4.96E+02	0.00E+00	0.00E+00	8.47E-06	1.20E-04	1.76E-04
53127	1.12E+02	0.00E+00	0.00E+00	1.95E-06	2.77E-05	3.97E-05
53129	4.01E+02	7.08E-02	1.77E-04	6.90E-06	9.78E-05	1.43E-04
54128	4.44E+00	0.00E+00	0.00E+00	7.70E-08	1.09E-06	1.58E-06
54129	2.54E-02	0.00E+00	0.00E+00	4.37E-10	6.19E-09	9.02E-09
54130	1.48E+01	0.00E+00	0.00E+00	2.53E-07	3.58E-06	5.26E-06



54131	1.25E+03	0.00E+00	0.00E+00	2.11E-05	2.99E-04	4.43E-04
54132	3.01E+03	0.00E+00	0.00E+00	5.06E-05	7.17E-04	1.07E-03
54134	4.41E+03	0.00E+00	0.00E+00	7.30E-05	1.04E-03	1.57E-03
54136	5.95E+03	0.00E+00	0.00E+00	9.71E-05	1.38E-03	2.11E-03
55133	3.26E+03	0.00E+00	0.00E+00	5.43E-05	7.70E-04	1.16E-03
55134	9.81E+00	1.27E+04	1.30E+03	1.63E-07	2.31E-06	3.49E-06
55135	1.48E+03	1.70E+00	1.15E-03	2.43E-05	3.44E-04	5.25E-04
55137	2.64E+03	2.30E+05	8.70E+01	4.28E-05	6.07E-04	9.40E-04
56134	4.07E+02	0.00E+00	0.00E+00	6.74E-06	9.55E-05	1.45E-04
56135	6.06E-01	0.00E+00	0.00E+00	9.96E-09	1.41E-07	2.15E-07
56136	3.79E+01	0.00E+00	0.00E+00	6.18E-07	8.76E-06	1.35E-05
56137	8.19E+02	0.00E+00	0.00E+00	1.33E-05	1.88E-04	2.91E-04
56138	3.76E+03	0.00E+00	0.00E+00	6.04E-05	8.56E-04	1.34E-03
57138	1.38E-02	3.41E-10	2.47E-08	2.22E-10	3.15E-09	4.92E-09
57139	1.55E+03	0.00E+00	0.00E+00	2.47E-05	3.51E-04	5.51E-04
58140	1.48E+03	0.00E+00	0.00E+00	2.34E-05	3.32E-04	5.26E-04
58142	1.44E+03	7.24E-11	5.04E-14	2.24E-05	3.18E-04	5.10E-04
59141	3.01E+03	0.00E+00	0.00E+00	4.73E-05	6.71E-04	1.07E-03
60142	3.76E+01	0.00E+00	0.00E+00	5.87E-07	8.32E-06	1.34E-05
60143	2.15E+03	0.00E+00	0.00E+00	3.34E-05	4.73E-04	7.64E-04
60144	1.08E+03	1.28E-09	1.19E-12	1.66E-05	2.36E-04	3.84E-04
60145	1.87E+03	7.69E-11	4.11E-14	2.86E-05	4.06E-04	6.65E-04
60146	9.42E+02	0.00E+00	0.00E+00	1.43E-05	2.03E-04	3.35E-04
60148	1.00E+03	0.00E+00	0.00E+00	1.50E-05	2.13E-04	3.56E-04
60150	2.21E+02	0.00E+00	0.00E+00	3.27E-06	4.63E-05	7.85E-05
61147	3.26E+01	3.03E+04	9.28E+02	4.93E-07	6.98E-06	1.16E-05
62147	7.26E+02	1.67E-05	2.30E-08	1.10E-05	1.55E-04	2.58E-04
62148	2.18E+02	6.64E-11	3.05E-13	3.26E-06	4.63E-05	7.74E-05
62149	6.95E+00	8.35E-12	1.20E-12	1.04E-07	1.47E-06	2.47E-06
62150	6.77E+02	0.00E+00	0.00E+00	1.00E-05	1.42E-04	2.41E-04
62151	1.92E+01	5.05E+02	2.63E+01	2.82E-07	4.00E-06	6.83E-06
62152	2.81E+02	0.00E+00	0.00E+00	4.11E-06	5.82E-05	1.00E-04
62154	4.55E+01	0.00E+00	0.00E+00	6.56E-07	9.30E-06	1.62E-05
63151	1.55E+00	0.00E+00	0.00E+00	2.28E-08	3.23E-07	5.51E-07
63152	1.35E-02	2.38E+00	1.77E+02	1.97E-10	2.79E-09	4.79E-09
63153	2.24E+02	0.00E+00	0.00E+00	3.24E-06	4.60E-05	7.95E-05
63154	1.88E+01	5.08E+03	2.70E+02	2.71E-07	3.84E-06	6.68E-06
63155	3.01E+00	1.48E+03	4.93E+02	4.30E-08	6.10E-07	1.07E-06
64152	8.96E-02	1.95E-12	2.18E-11	1.31E-09	1.86E-08	3.19E-08
64154	2.70E+01	0.00E+00	0.00E+00	3.90E-07	5.52E-06	9.61E-06

64155	1.00E+01	0.00E+00	0.00E+00	1.44E-07	2.04E-06	3.57E-06
64156	9.15E+01	0.00E+00	0.00E+00	1.30E-06	1.85E-05	3.25E-05
64157	1.09E-01	0.00E+00	0.00E+00	1.54E-09	2.19E-08	3.88E-08
64158	3.17E+01	0.00E+00	0.00E+00	4.45E-07	6.30E-06	1.13E-05
64160	1.60E+00	0.00E+00	0.00E+00	2.21E-08	3.14E-07	5.67E-07
65159	3.39E+00	0.00E+00	0.00E+00	4.74E-08	6.72E-07	1.21E-06
66160	1.50E-01	0.00E+00	0.00E+00	2.07E-09	2.94E-08	5.31E-08
66161	4.34E-01	0.00E+00	0.00E+00	5.98E-09	8.48E-08	1.54E-07
66162	3.19E-01	0.00E+00	0.00E+00	4.37E-09	6.19E-08	1.13E-07
66163	1.64E-01	0.00E+00	0.00E+00	2.23E-09	3.17E-08	5.83E-08
66164	3.58E-02	0.00E+00	0.00E+00	4.85E-10	6.87E-09	1.27E-08
67165	5.68E-02	0.00E+00	0.00E+00	7.64E-10	1.08E-08	2.02E-08
68166	1.52E-02	0.00E+00	0.00E+00	2.03E-10	2.88E-09	5.41E-09
68167	1.35E-03	0.00E+00	0.00E+00	1.79E-11	2.54E-10	4.80E-10
68168	2.71E-03	0.00E+00	0.00E+00	3.59E-11	5.08E-10	9.65E-10

## APPENDIX B

Reactor core specifications [8].

Details	Material	Dimensions	Remarks
<b>Fuel Rod Specifications</b>			
Pellet Radius	UO <sub>2</sub> / UO <sub>2</sub> + PuO <sub>2</sub> / TRU	0.4095 cm	
Pitch		1.26	
Clad Inner Radius	Zirc-Alloy4	0.4177 cm	
Clad Outer Radius		0.475 cm	
Fuel Stack Height		244 cm	
Rod Height		305cm	
<b>Pyrex Rod Specifications</b>			
Inner Tube Inner Radius	SS304	0.214 cm	B-10 Loading: 6.535 mg/cm
Inner Tube Outer Radius		0.231 cm	
Pyrex Rod Inner Radius	Borosilicate Glass	0.241 cm	
Pyrex Rod Outer Radius		0.427 cm	
Outer Clad Inner Radius	SS304	0.437 cm	
Outer Clad Outer Radius		0.484 cm	
<b>IFBA Specifications</b>			
Boron Coating Thickness	ZrB <sub>2</sub>	17 μm	B-10 Loading: 2.355 mg
<b>WABA Specifications</b>			
Inner Clad Inner Radius	Zirc-Alloy4	0.2858 cm	
Inner Clad Outer Radius		0.339 cm	
Pyrex Rod Inner Radius	B <sub>4</sub> C-Al <sub>2</sub> O <sub>3</sub>	0.3531 cm	B-10 Loading: 6.165 mg/cm
Pyrex Rod Outer Radius		0.4039 cm	
Outer Clad Inner Radius	Zirc-Alloy4	0.418 cm	

Outer Clad Outer Radius		0.4839 cm	
RCCA Specifications			
Poison Radius		0.525 cm	For Ag-In Cd Rods: 80% Ag, 15% In and 5% Cd ( $\rho = 10.2$ g/cc)
Poison Height		290-300 cm	
Step Size	Ag-In-Cd / B <sub>4</sub> C	1.5875 cm	
Number of Steps		183 Nos.	For B <sub>4</sub> C Rods: 95% B and 5% C ( $\rho = 2.016$ g/cc)
Pressure Vessel Specifications			
Vessel Inner Radius		142.7 cm	
Vessel Outer Radius	SS316	147.7 cm	

## APPENDIX C

Isotopic composition for clad, structural, control rod, core barrel and reactor vessel.

Details	w/o / Atomic Density	Remarks
Burnable Poisons		
PYREX Rod		
B <sup>10</sup>	0.74 %	80% SiO <sub>2</sub> , 13% B <sub>2</sub> O <sub>3</sub> , 4% Na <sub>2</sub> O, 3% Al <sub>2</sub> O <sub>3</sub>  ρ = 2.25 g/cm <sup>3</sup>
B <sup>11</sup>	3.29 %	
Si <sup>28</sup>	34.36 %	
Si <sup>29</sup>	1.80 %	
Si <sup>30</sup>	1.24 %	
Na <sup>23</sup>	2.97 %	
Al <sup>27</sup>	1.58 %	
O <sup>16</sup>	54.01 %	
IFBA Rod		
B <sup>10</sup>	3.53 %	ZrB <sub>2</sub>  ρ = 6.085 g/cm <sup>3</sup>
B <sup>11</sup>	15.62 %	
Zr <sup>90</sup>	40.99 %	
Zr <sup>91</sup>	9.04 %	
Zr <sup>92</sup>	13.96 %	
Zr <sup>94</sup>	14.46 %	
Zr <sup>96</sup>	2.38 %	
WABA Rod		
B <sup>10</sup>	1.968 %	Al <sub>2</sub> O <sub>3</sub> – B <sub>4</sub> C  ρ = 2.593 g/cm <sup>3</sup>
B <sup>11</sup>	8.992 %	
C	3.04 %	
Al <sup>27</sup>	45.521 %	
O <sup>16</sup>	40.479 %	
Control Rods		
Silver-Indium-Cadmium		
Ag <sup>107</sup>	2.3523e-2 /barns-cm	80% Ag, 15% In, 5% Cd  ρ = 10.16 g/cm <sup>3</sup>
Ag <sup>109</sup>	2.1854e-2 /barns-cm	
Cd <sup>106</sup>	3.4019e-5 /barns-cm	
Cd <sup>108</sup>	2.4221e-5 /barns-cm	
Cd <sup>110</sup>	3.3991e-4 /barns-cm	

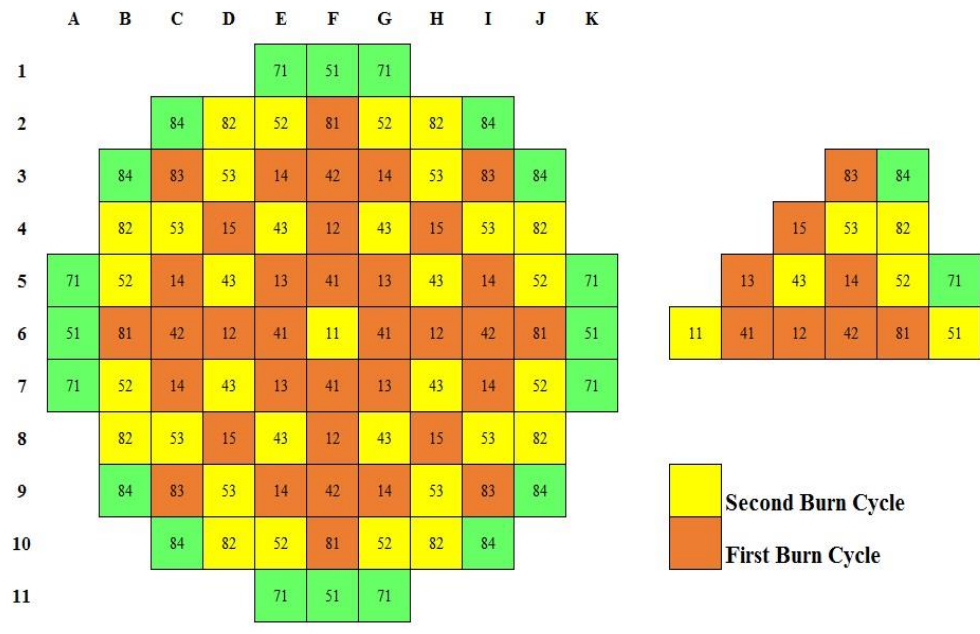
Cd <sup>111</sup>	3.4835e-4 /barns-cm	
Cd <sup>112</sup>	6.5669e-4 /barns-cm	
Cd <sup>113</sup>	3.3257e-4 /barns-cm	
Cd <sup>114</sup>	7.8188e-4 /barns-cm	
Cd <sup>116</sup>	2.0384e-4 /barns-cm	
In <sup>113</sup>	3.4291e-4 /barns-cm	
In <sup>115</sup>	7.6504e-3 /barns-cm	
<b>Boron Carbide</b>		
B <sup>10</sup>	18.905 %	B <sub>4</sub> C $\rho = 2.016 \text{ g/cm}^3$
B <sup>11</sup>	76.095 %	
C	5 %	
<b>Clad</b>		
Zr	98.23 %	Zircaloy4 $\rho = 6.52 \text{ g/cm}^3$
Fe	0.21 %	
Sn	1.45 %	
Cr	0.1 %	
Hf	0.01 %	
<b>Guide Tube</b>		
C	0.08 %	SS 304 $\rho = 7.8 \text{ g/cm}^3$
P <sup>31</sup>	0.045 %	
Si <sup>28</sup>	0.75 %	
Ni <sup>58</sup>	8 %	
Mn <sup>55</sup>	2 %	
S <sup>32</sup>	0.03 %	
Cr <sup>52</sup>	18 %	
N <sup>14</sup>	0.1 %	
Fe <sup>56</sup>	70.995 %	
<b>Core Barrel and Reactor Vessel</b>		
Cr <sup>52</sup>	16 %	SS 316 $\rho = 7.99 \text{ g/cm}^3$
Ni <sup>58</sup>	10 %	
Mn <sup>55</sup>	2 %	
Si <sup>28</sup>	0.75 %	
N <sup>14</sup>	1 %	
C	0.08 %	



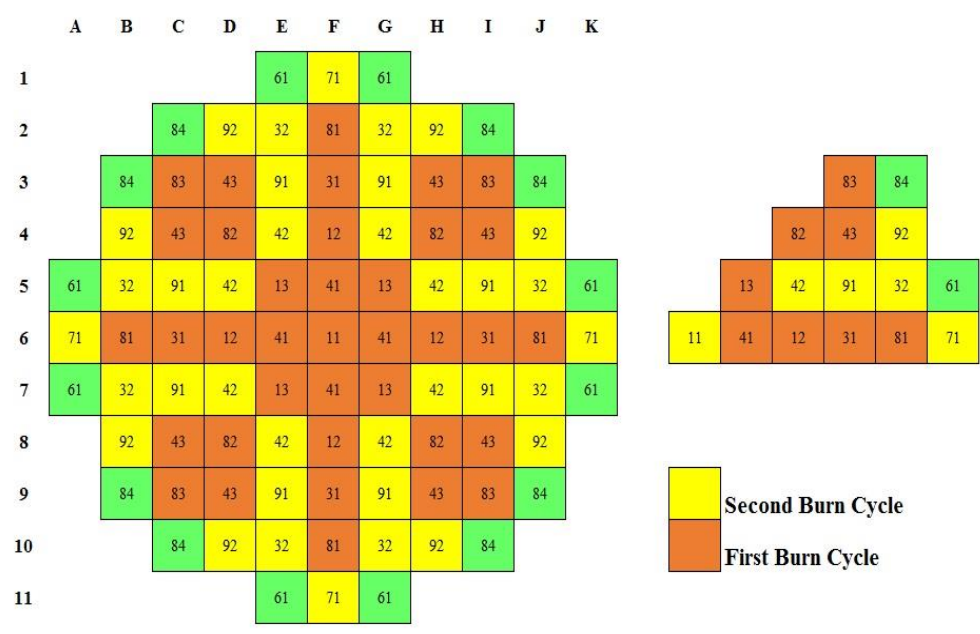
P <sup>31</sup>	0.045 %	
S <sup>32</sup>	0.03 %	
Mo <sup>98</sup>	2 %	
Fe <sup>56</sup>	68.995 %	

## APPENDIX D

Three batch refueling arrangement for UOX-1/21-2.35/16-3.4/52-4.45  
and UOX-2/09-2.35/32-3.4/48-4.45



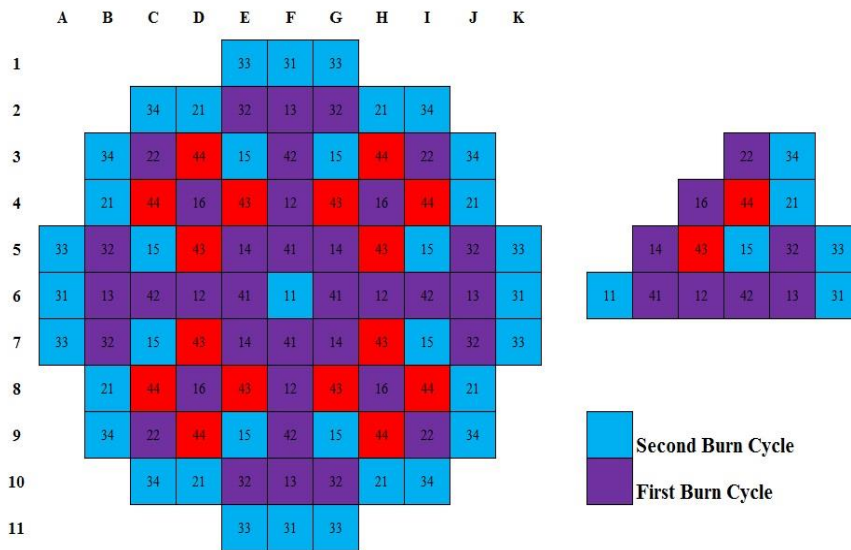
UOX-1/21-2.35/16-3.4/52-4.45



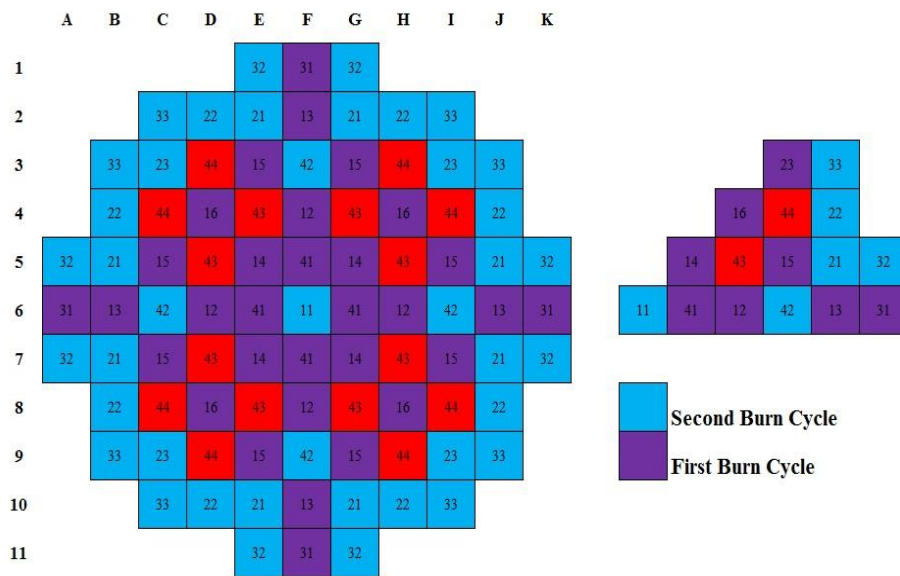
UOX-2/09-2.35/32-3.4/48-4.45

## APPENDIX E

Three batch refueling arrangement for MOX-1 / RG / 25-4.5/40-4.2 /24-MOX and MOX-2 / WG / 25-4.5/40-4.2 /24-MOX core.



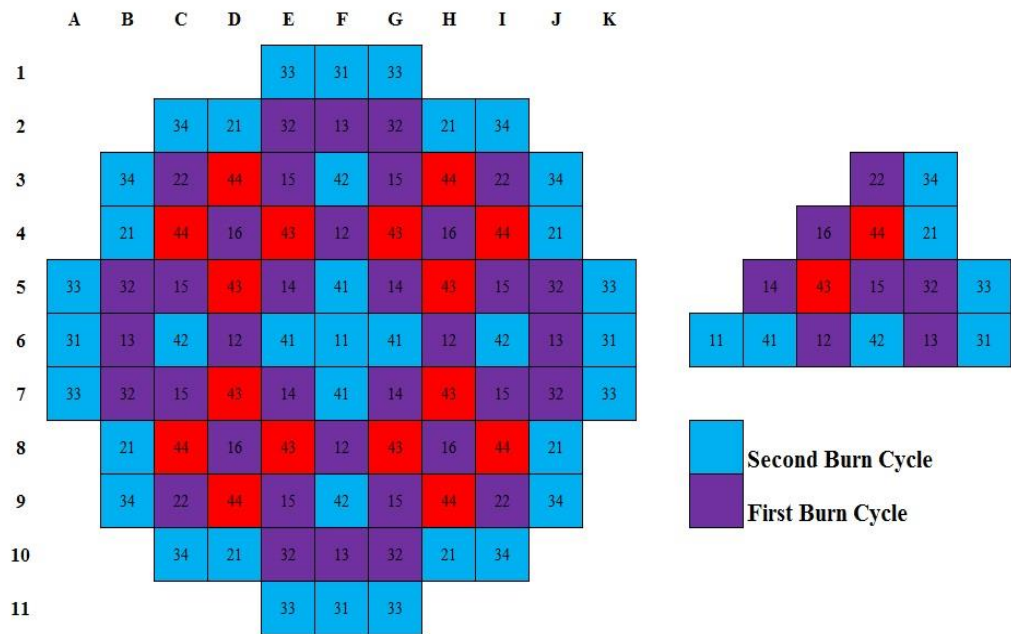
MOX-1/RG/25-4.5/40-4.2/24-MOX



MOX-1/WG/25-4.5/40-4.2/24-MOX

## APPENDIX F

Three batch refueling arrangement for TRU-1 /25-4.5/40-4.2 /24-TRU core.



TRU-1/25-4.5/40-4.2/24-TRU

## BIBLIOGRAPHY

1. Richard Rhodes and Denis Beller. Foreign Affairs. <http://www.foreignaffairs.com/articles/55629/richard-rhodes-and-denis-beller/the-need-for-nuclear-power>. (Accessed 20<sup>th</sup> Feb 2015).
2. John E. Earp. 2013. Briefing – Small Modular Reactors.
3. Nuclear Regulation Committee. Small Modular Reactors. <http://www.nrc.gov/reactors/advanced/smr.html>. (Accessed 26<sup>th</sup> Feb 2015).
4. Nuclear Energy Association (NEA), June 2011. Current Status, Technical Feasibility and Economics of Small Modular Reactors.
5. Westinghouse. Small Modular Reactors. <http://www.westinghousenuclear.com/New-Plants/Small-Modular-Reactor>. (Accessed 28<sup>th</sup> Feb 2015).
6. International Atomic Energy Association (IAEA). September 2011. Status of Small and Medium Sized Reactors.
7. Alexander W. Harkness. Westinghouse Electric Company. June 2013. Westinghouse Small Modular Reactor.
8. Consortium for Advanced Simulation of LWRs (CASL). March 2013. VERA Core Physics Benchmark Progression Problem Specifications
9. David E. Ames II et al. Sandia National Laboratory. High Fidelity Nuclear Energy System Optimization towards an Environmentally Benign, Sustainable and Secure Energy Source.
10. Tomasz Kozlowski and Thomas J. Downar. December 2003. OECD/NEA AND U.S. NRC PWR MOX/UO<sub>2</sub> Core Transient Benchmark.
11. Reed Robert Burn. December 1988. Introduction to Nuclear Reactor Operations. Reactor Core Analysis Chapter 9.
12. Reactor Kinetics. [http://nuclearpowertraining.tpub.com/h1019v2/css/h1019v2\\_104.htm](http://nuclearpowertraining.tpub.com/h1019v2/css/h1019v2_104.htm).
13. Oak Ridge National Laboratory. MCNPX Manual Volume II.
14. Energy Information Administration. February 1995. Spent Nuclear Fuel Discharges from US Reactors



15. M. J. Driscoll et al. American Nuclear Society, La Grange Park, Illinois. 1990. The Linear Reactivity Model for Nuclear Fuel Management.

## VITA

Brendan Dsouza was born on 4<sup>th</sup> October 1988 in Mumbai, India. He graduated from University of Mumbai in May 2010 with a Bachelor's degree in Mechanical Engineering. He worked for three years in India as a QA-QC Engineer for projects associated with Indian Oil Corporation Ltd. (IOCL) and Hindustan Petroleum Corporation Ltd. (HPCL). He enrolled at Missouri University of Science and Technology in fall 2013 for the Master's program in Nuclear Engineering. In May, 2015, he received his Master's degree in Nuclear Engineering from Missouri University of Science and Technology.